Received: 7 February 2022 | Revised: 28 April 2022 | Accepted: 2 May 2022

DOI: 10.1111/1541-4337.12983

COMPREHENSIVE REVIEWS IN FOOD SCIENCE AND FOOD SAFETY

Comprehensive REVIEWS in Food Science and Food Safety WILEY

Hyperspectral imaging and machine learning in food microbiology: Developments and challenges in detection of bacterial, fungal, and viral contaminants

Aswathi Soni[1] | **Yash Dixit**[2] | **Marlon M. Reis**[2] | **Gale Brightwell**[1,3]

[1]Food System Integrity, Consumer Food Interface, AgResearch Ltd, Palmerston North, New Zealand

[2]Food Informatics, Smart Foods, AgResearch Ltd, Palmerston North, New Zealand

[3]New Zealand Food Safety Science Research Centre, Palmerston North, New Zealand

Correspondence
Aswathi Soni, Food System Integrity, Hopkirk Research Institute, Corner University Avenue & Library Road, Massey University, Palmerston North 4414, New Zealand.
Email: aswathi.soni@agresearch.co.nz

Funding information
AgResearch Ltd. Strategic Science Investment Fund, Grant/Award Number: (A25768)

Abstract

Hyperspectral imaging (HSI) is a robust and nondestructive method that can detect foreign particles such as microbial, chemical, and physical contamination in food. This review summarizes the work done in the last two decades in this field with a highlight on challenges, risks, and research gaps. Considering the challenges of using HSI on complex matrices like food (e.g., the confounding and masking effects of background signals), application of machine learning and modeling approaches that have been successful in achieving better accuracy as well as increasing the detection limit have also been discussed here. Foodborne microbial contaminants such as bacteria, fungi, viruses, yeast, and protozoa are of interest and concern to food manufacturers due to the potential risk of either food poisoning or food spoilage. Detection of these contaminants using fast and efficient methods would not only prevent outbreaks and recalls but will also increase consumer acceptance and demand for shelf-stable food products. The conventional culture-based methods for microbial detection are time and labor-intensive, whereas hyperspectral imaging (HSI) is robust, nondestructive with minimum sample preparation, and has gained significant attention due to its rapid approach to detection of microbial contaminants. This review is a comprehensive summary of the detection of bacterial, viral, and fungal contaminants in food with detailed emphasis on the specific modeling and datamining approaches used to overcome the specific challenges associated with background and data complexity.

KEYWORDS
bacteria, detection, food safety, hyperspectral imaging, modeling, virus

1 | INTRODUCTION

Foodborne microbial contaminants include bacteria, viruses, fungi, yeast, and protozoa that can either cause food poisoning and diseases associated, or lead to spoilage of the food products, thereby reducing their shelf life (Martinović et al., 2016; Zastempowska et al., 2016). Foodborne pathogens include specific bacterial species consisting of spore-forming and nonspore-forming strains, which can either produce preformed toxins in the food or inside the human body (intestine) and lead to several types of mild to severe symptoms in consumers. Some examples are *Clostridium perfringens*, *Campylobacter* spp., *Listeria monocytogenes*, *Vibrio parahaemolyticus*, *Bacillus cereus*, and *Escherichia coli* (Banerji et al., 2021; Vieira et al., 2021). Bacterial contaminants associated with food spoilage and foodborne outbreaks have been investigated and reported (Table 1).

Not all the bacterial species associated with food spoilage are related to pathogenicity. For example, *Brochothrix thermosphacta*, *Lactobacillus* spp., *Carnobacterium* spp., *Lactococcus* spp., *Leuconostoc* spp., *Pediococcus* spp., *Streptococcus* spp., *Kurthia zopfii*, *Clostridium* spp., *Bacillus* spp., and *Weisella* spp. are associated with food spoilage, thereby causing off-odors and other organoleptic changes in food products (Lorenzo et al., 2018). *Pseudomonas fluorescens*, *Pseudomonas putida*, *Pseudomonas fragi*, and *Pseudomonas perolens* have also been reported to be associated with food spoilage, especially at refrigerated temperatures, often linked to blue pigment formation and off-odors in cheese, as well as proteolysis and off odors in unpasteurized milk (Martin et al., 2011; Raposo et al., 2016). *B. thermosphacta* is a known spoiler of meat products, resulting in off-flavors, discoloration, and gas production in beef, pork, chicken, and fish (Gardner, 1981; Xu et al., 2010). Other bacteria associated with food spoilage are *Zymomonas mobilis* in beverages (Jespersen & Jakobsen, 1996), *Shewanella putrefaciens* in fish (Gram & Melchiorsen, 1996), and *Photobacterium phosphoreum* in fish and pork (Dalgaard et al., 1997; Nieminen et al., 2016).

Foodborne fungi and yeast are also associated with the spoilage of food products as well as food poisoning. Fungi can be classified into two types based on their role in food: beneficial types include edible fungi (e.g., mushrooms), medicinal varieties (*Penicillium chrysogenum* and *Penicillium nalgiovense*), fermenters, and citric acid producers (e.g., *Aspergillus niger*) (Turner et al., 2012). On the other hand, toxic fungi that produce mycotoxins and aflatoxins are a concern for public health authorities (F. Wu et al., 2014). Mycotoxins are secondary metabolites produced by some species of fungi that are capable of causing risks to human health including cancer, growth interruptions, immune suppression, and neural tube defects (Bennett & Klich, 2003). Aflatoxins, ochratoxins, fumonisins, deoxynivalenol, and alterotoxins are some examples of mycotoxins that can cause acute or chronic toxicity in humans and animals (Alshannaq & Yu, 2017; H. B. Lee et al., 2015). Table 2 summarizes the food safety concerns due to fungi.

Some fungal species associated with food spoilage are *Paecilomyces fulvus*, *Paecilomyces niveus*, *Penicillium expansum*, *Penicillium roqueforti*, *Galactomyces* spp., *Aspergillus* spp., *Rhizopus* spp., and *Xeromyces bisporus* (Saleh & Al-Thani, 2019; Snyder et al., 2019). Some other fungal contaminants such as *Alternaria, Aspergillus, Candida, Fusarium*, and *Mucormycetes* spp. are pathogenic in nature and can lead to moderate to severe symptoms in immunocompromised individuals (Benedict et al., 2016) (Table 2). Fungal food spoilage has been extensively reviewed by various researchers (Dagnas & Membré, 2013; Garnier et al., 2017; Kure & Skaar, 2019; Snyder & Worobo, 2018). The contamination of fungi in food is largely attributed to the mishandling of food, storage conditions, humidity, and water activities of the storage units and can be mainly controlled by good manufacturing hygiene practices.

Foodborne viruses (Table 3) need host cells to replicate (Stals et al., 2012). Although viruses cannot use food molecules as host cells to replicate, they can use food as a potential carrier and are known to remain stable in food matrices (Koopmans & Duizer, 2004). The emerging risk of new variants of viruses calls for preventive actions that can enable early detection. This will be a primary step toward mitigation. The mechanism of infection by viruses involves the production of virions. This step needs access to a human or animal cell, through invasion of the plasma membrane of a target cell, followed by exploitation of the organelles in the host cell systems for replication and secretion of proteins (Louten, 2016). Foodborne transmission could be one of the modes in the epidemiology of viruses, especially with norovirus, rotavirus, hepatitis E, and hepatitis A. Foodborne viruses are transmitted due to the excretion of high numbers in the feces or through emesis, have low infectious doses, and are capable of withstanding the processing regimes, which further adds to the risk of contamination and food poisoning (Bosch et al., 2018). Therefore, techniques of early detection as a part of a prevention plan could prove useful. There is a research gap and lack of complete understanding of behaviors, infective capability and resistance of foodborne viruses under various conditions such as low pH, moisture, heat, disinfectants, and thermal processing. Viruses that have been reported to contaminate food and influence either shelf life or food safety are listed in Table 3.

TABLE 1 Common foodborne bacterial pathogens, related concerns, and specific food items that have been reported to be contaminated

Bacterial strain/strains	Food safety or related concerns	Food items reported to be contaminated	References
Campylobacter jejuni	Diarrhea (often bloody), fever, stomach cramps, irritable bowel syndrome, temporary paralysis, and arthritis in immunocompromised individuals	Undercooked or raw chicken, beef, and pork, unpasteurized milk	(Jacobs-Reitsma et al., 2008; Sibanda et al., 2018)
Salmonella enterica serovar Typhimurium, *Salmonella infantis, Salmonella typhi, Salmonella* Enteritidis	Diarrhea, vomiting, and abdominal cramps. Fatality reported in immunocompromised individuals	Eggs, chicken, fresh vegetables, and red meat	(Duguid & North, 1991; Meyer et al., 2010; Saw et al., 2020; Soltan Dallal et al., 2014)
Escherichia coli (STEC)	Travelers' diarrhea, hemolytic uremic syndrome (HUS) after 3 days of the onset of diarrhea	Raw milk, ground beef, and raw meat	(Armstrong et al., 1996; Oliver et al., 2009; Tuttle et al., 1999)
Listeria monocytogenes	Listeriosis is often associated with septicemia, meningitis, gastroenteritis, pneumonia, and spontaneous abortion with a mortality rate of 20–30% in immunocompromised individuals	Vegetables, milk, and raw refrigerated meat and poultry products	(Beuchat, 1996; Jami et al., 2014; Lovett et al., 1987; Ryser et al., 1996; Vázquez-Boland et al., 2001)
Bacillus cereus	Food-borne diarrhea: emetic and diarrheal syndromes, and a variety of local and systemic infections	Vegetables, milk, meat, spices, rice, and dried powder food	(Ankolekar et al., 2009; Griffiths & Schraft, 2017; Pei et al., 2018; Rusul & Yaacob, 1995)
Staphylococcus aureus	Food-borne diarrhea, toxic shock syndrome, scalded skin syndrome in infants and children, leucocytosis with necrotic lesions	Meat, ready-to-eat (RTE) food, milk, and vegetables	(Akindolire et al., 2015; Argudín et al., 2010; De Boer et al., 2009; Fueyo et al., 2005; Oh et al., 2007; Seo et al., 2010)
Clostridium botulinum	Neurotoxins (A–G dependent on the producing organism) can lead to blurred vision. Flaccid paralysis of the respiratory muscles and death	Inadequately processed and canned food, seafood, and minimally cooked chilled foods	(Peck, 2006)

TABLE 2 Common foodborne fungal pathogens, related concerns, and specific food items that were reported to be contaminated

Fungal strain	Foodborne effects	Food items reported to be contaminated	References
Aspergillus flavus, *Aspergillus parasiticus*, and *Aspergillus nomius (Aflatoxin M1)*	Carcinogenic, hepatotoxic, teratogenic, and mutagenic effects	Cereals-maize and rice	(Makun et al., 2011; Zöllner & Mayer-Helm, 2006)
Aspergillus flavus (Aflatoxin A1)	Carcinogenicity and immunosuppression	Medical plants considered edible: *Alyssicarpus vaginalis* and *Aerva lanata*	(Abeywickrama & Bean, 1991; Marchese et al., 2018)
Aspergillus spp. (Aflatoxin B1)	Oesophagal and gastric cancer development	Milk	(Veldman et al., 1992)
Saccharomyces cerevisiae strains are classified as opportunistic pathogens	Systemic infection leading to fatality in immunocompromised individuals	Bread, alcoholic beverages—beer and wine.	(Pérez-Torrado & Querol, 2016)
Penicillium expansum	Blue mold rot, which is a postharvest disease in apples	Apples during the storage	(Okull et al., 2006)
Penicillium roqueforti and *Penicillium commune*	Food spoilage	Generation of off-odor and unfavorable sensory attributes.	(Kure & Skaar, 2019)
Fusarium spp.	Fusarium head blight disease in grains and production of mycotoxins (zearalenone and fumonisin)	Infected grains are of low mass and shrunken	(McCormick, 2003)

TABLE 3 Common foodborne viral pathogens, related concerns, and specific food items that were reported to be contaminated

Viral strain	Foodborne effects	Food items reported to be contaminated	References
Norovirus	Foodborne gastroenteritis including vomiting and diarrhea with acute onset	Raw or undercooked oysters, herbs, vegetables, and fruits,	(Iritani et al., 2014)
Sapovirus	Etiologic agents of human gastroenteritis, diarrhea, abdominal pain, chills, vomiting, malaise fever, and headaches	Clam, oyster, contaminated lunch packs with multiple food products-without specific identification	(Hansman et al., 2007; Kobayashi et al., 2012)
Nipah virus	Respiratory and neurological symptoms ranging from asymptomatic infection to fatal encephalitis	Pork and a traditional liquor made from date palm	(Ang et al., 2018; Islam et al., 2016; Parashar et al., 2000)
Ebola virus	Ebola virus disease (EVD)	Bushmeat—meat from wildlife (e.g., monkeys and bats) slaughtered and prepared for human consumption	(Kodish et al., 2019; Onyekuru et al., 2020)
Hepatitis A virus (HAV)	Jaundice, fever, anorexia, nausea, vomiting, diarrhea, myalgia, and malaise	Shellfish, fruits, and salads	(Acheson & Fiore, 2004)
Hepatitis E virus (HEV)	Acute symptoms like myalgia, arthralgia, weakness, and vomiting resembling flu. Severe symptoms lead to chronic liver diseases and fulminant hepatic failure.	Swine, chicken, and deer meat	(Van der Poel, 2014; Wedemeyer et al., 2012)

2 | CONVENTIONAL METHODS USED FOR THE DETECTION OF BACTERIA, FUNGI, AND VIRUSES

Conventional methods for the detection of bacteria in food samples are based on culturing the microorganisms on solid media (agar plates) or in liquid media (nutrient broths) depending on the sample type, followed by biochemical identification. For more specific bacterial groups, selective media plates and specific conditions are used for eliminating the interference of any background flora. Some of the detection protocols include a step of enrichment, which is described as providing a nonselective nutrient-rich medium for bacteria or fungi in low numbers to proliferate, followed by detection using routine methods. These conventional culture-based methods can take anywhere from 3 days to 1 week for a presumptive result. A significant reduction in the time required for detection of bacterial pathogens and spoilage bacteria is achieved by nucleic acid-based methods (polymerase chain reaction [PCR], real-time or quantitative PCR [qPCR], multiplex PCR [mPCR], immunological methods (Enzyme-linked immunosorbent assay [ELISA] and lateral flow immunoassays) and biosensor-based methods such as optical biosensors, electrochemical biosensors and mass-based biosensors (bulk acoustic wave resonators [BAW] or quartz crystal microbalance [QCM]; Law et al. (2014)).

The standard methods to detect fungal contamination in food use culture-dependent methods, which are time, labor, and consumable-intensive and have limitations on detection based on certain culture conditions. Mycotoxins in food are detected through techniques such as high-performance liquid chromatography (HPLC) with specialized detectors such as fluorescence, diode array, UV, and mass spectrometry (MS) (Agriopoulou et al., 2020). Recently, the electronic nose has also been investigated as a tool to detect the volatiles generated by some fungi species in food, which could help in identification (Suchorab et al., 2019). However, the use of volatile profiling has been predominantly investigated in nonfood matrices as food can add complexities due to the presence and degradation of biomolecules.

The infectious dose of most foodborne viruses, such as norovirus or hepatitis A virus, is 10–100 infectious particles, which indicates the requirement of extensive sensitivity in the detection methods (Bosch et al., 2011). Techniques based on the amplification of nucleic acids, such as sequence-based amplification, loop-mediated isothermal amplification, and reverse transcription-polymerase chain reaction (RT-PCR) are commonly used (Pintó & Bosch, 2008). The culture-based techniques for the detection of viruses are time-consuming, requiring a series of

concentration and purification steps to elute viruses from the food matrix while ensuring the virus infectivity is not affected, followed by using cell lines for detection (Bosch et al., 2011; Cliver et al., 1983). The time required for these culture-based techniques could be attributed to the need for optimization for each strain.

3 | HYPERSPECTRAL IMAGING: THE STATE OF THE ART

Hyperspectral imaging (HSI) is a nondestructive technique with applications in food safety including the detection of adulterations, as well as microbial, chemical, and physical contamination in food. HSI is a combination of conventional imaging and spectroscopy, in which a spectrum for each point (i.e., pixel) in an area of interest in the sample being analyzed is obtained (Gowen et al., 2007). The spectroscopic component of HSI can involve spectral ranges from ultraviolet (UV) to Terahertz, but the most common are visible (VIS) and near-infrared (NIR) (Penner, 2017). The design of the spectroscopic system used to acquire the spectrum for each pixel is dependent on the devices being used to scan the area of interest and spectral range (Ren et al., 2014; Wu & Sun, 2013). The system used to scan the area of interest can involve two approaches: (1) a nonstatic approach where only a point or a line in the sample is scanned at a time or (2) a static system, where the whole area is scanned at once. Several techniques exist for the static system, where either each wavelength in the spectral range of interest is scanned at a time or filters are placed on the sensor to detect the specific wavelength of interest. Thus, the optical system needs to direct the light coming out of the sample into the detection system. An HSI system essentially consists of a light source, a hyperspectral camera, and a computer for data acquisition. Generally, the HSI camera consists of imaging optics, a narrow slit, a diffraction grating, and a 2D focal plane array (FPA) detector (typically charge-coupled device CCD or complementary metal-oxide-semiconductor [CMOS]). The sample is illuminated via a light source and then the image is projected through the slit onto the diffraction grating where the light is split into discrete wavelengths and physically separated followed by projection onto the FPA. One dimension of the FPA corresponds to the wavelength of light, while the other dimension corresponds to the "vertical" position along the slit. At each X–Y coordinate, a pixel is energized to a certain level, depending on the intensity of the light at that position and wavelength (Gibbons, 2014; Rodrigues et al., 2020). Finally, it produces a stack of images, at a wide range of contiguous wavelengths (intervals of < 10 nm), and every pixel in the hyperspectral image has an individual spectrum over a wide range of contiguous wavelengths (Wu & Sun, 2013). HSI provides various advantages over multispectral imaging (MSI) such as a broader wavelength range with narrower bands, higher sensitivity to minor components as well as broader multiconstituent information (Gowen et al., 2007). HSI systems are commercially available in different electromagnetic spectral regions: ultraviolet-visible (UV-Vis), visible–near-infrared (Vis-NIR), near-infrared (NIR), short-wavelength infrared (SWIR), medium wavelength infrared (MWIR), and long-wavelength infrared (LWIR).

The techniques used for image acquisition are commonly described as:

1. Point scanning: In this method, a single point of location on the sample is scanned at one pixel to generate a spectrum, while the other points are scanned by moving either the detector or the sample along two spatial dimensions (x and y). This method is also known as the whiskbroom method (Wu & Sun, 2013).
2. Line scanning: This method is also known as the push broom method where a whole line on the sample is exposed to the light and spectral information corresponding to each spatial pixel in the line is obtained. Line scanning is the preferred method of acquiring HSI in food-based samples in processing lines due to its suitability to adapt to conveyer belt-like systems.
3. Area scanning: This method (band sequential method or wavelength scanning) uses a fixed view to obtain a two-dimensional monochrome image using the x- and y-axis, along with full spatial information at one wavelength per attempt. The process is repeated over the whole wavelength range to acquire a stack of single band images stored in the band sequential (BSQ) format.
4. Single-shot (snapshot) method: This method can record both spatial and spectral information with a single exposure and convert it into a compressed hyperspectral image (He et al., 2020).

Out of all the methods, HSI using line-scanning is most frequently used and reported in food-based applications (Gowen et al., 2007; Liu et al., 2017; Marshall et al., 2015; Siche et al., 2016), and therefore, this topic has not been revisited in this review. A hyperspectral image is a three-dimensional (3D) cubical composition generated by the two-dimensional (2D) spatial and one-dimensional (1D) spectral information with a high level of spectral resolution (Ren et al., 2014; Wu & Sun, 2013). The cubical composition or hypercube is also referred to as a spectral cube, spectral volume, data cube, and data volume by various researchers. Figure 1 illustrates a typical postprocessing workflow after a hypercube is obtained. In the last 10 years, researchers have started exploring and utilizing the spatial

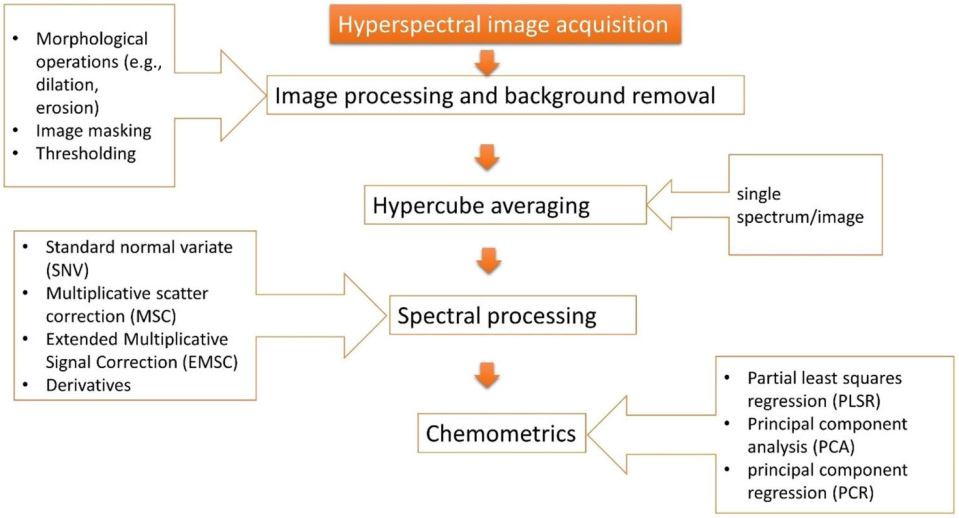

FIGURE 1 Typical postprocessing workflow after hypercube acquisition

aspect of HSI with greater success, which can be observed in the current review.

HSI technique is based on the detection of spectral changes of broadband light after it interacts with the sample. The spectrum of original broadband light is characterized by standards with known reflectance, producing the "white reference spectrum," which is defined as 100% of reflectance. In addition to the white reference spectrum, a dark reference spectrum is also utilized, that measures the spectrum of the system without the presence of the broadband light, which is considered the 0% reflectance. The use of these two types of reference allows for the correction of variation in the instrumental system. Spectroscopy in Vis-NIR regions has demonstrated success with food products through quality-associated changes. Most of the changes are attributed to modifications in functional groups like CH, NH, and OH, which lead to the overtone and combination vibrations in Vis-NIR spectral region (Magwaza et al., 2012; Pu et al., 2015). A similar approach using the functional groups in the chemical composition of microbial structures requires high sensitivity and precision followed by processing software to distinguish and filter false positives and false negatives from the results. However, there are challenges associated with using the big data generated by this technology as well as limitations on the identification of microbial species in real complex matrices.

3.1 | Importance of spectral range selection

The data obtained from HSI are known to have a high dimensionality with redundancy between adjacent wavelengths; therefore, using all the wavebands in the application is not necessary. This warrants wavelength selection, which is achieved by using one or more algorithms/models such as partial least squares regression (PLSR), least-squares support vector machines (LS-SVM), projections algorithm (SPA), loading weights (LW), regression coefficients (RC), and so forth to select a few essential wavelengths, which carry the most useful spectral information that is related to the spectral signatures of the target components (Xia et al., 2017; X. Zhang et al., 2013). The wavelength range to be used for a particular purpose is critical, which defines the ability of the HSI system to capture the relevant spectral features of the target. A study by Feng et al. (2018) compared various variable selection algorithms namely, competitive adaptive reweighted sampling (CARS), SPA, and genetic algorithm (GA) for the optimized wavelength selection classification of bacterial colonies on the agar plate. SPA yielded the best overall correct classification rates as compared to the others (Feng et al., 2018). Similarly, for the detection of moisture in food products, absorption bands near 1400−1440 nm and 1900 to 1950 nm have often been used (Büning-Pfaue, 2003). Absorption peaks around 970 nm, 1190 nm, 1450 nm, and 1940 nm arise due to the second overtone of the OH-stretching band, the combination of the first overtone of the OH-stretching and the OH-bending band, the first overtone of the OH-stretching band and combination of the OH-stretching band and the OH-bending band, respectively (Büning-Pfaue, 2003). In simple words, the wavelength region allows capturing the fundamental peaks related to the target attribute such as moisture, dryness, or specific compositional element that could indirectly be linked to bacterial spoilage. Moisture could be a direct measurement of food quality (Arefi et al.,

2021) or could be used as an indicator of other processes such as drying (Crichton et al., 2018). In another example, for detecting total viable count (TVC) in pork samples, the required wavelength range covered visible (400–700 nm), and/or NIR with peaks related to fat (around 900 and 1200 nm) and/or other nutrients such as glycogen or protein. As the bacterial spoilage increases in pork, the change in the color of meat and the composition of nutrients can potentially be captured via HSI (Huang et al., 2013; Kong & Ma, 2003). Similar examples are captured in Tables 4–8, indicating wavelength range used for various studies.

This review summarizes publications in the last two decades that reported the success and challenges in using HSI as a useful technique in food microbiology. The review also discusses the recent developments in the use of deep learning to address these limitations. However, the development of deep learning models has significantly increased the potential of HSI and data interpretation. The paper also discusses the research gaps, which could benefit from further research and development of HSI with data processing mitigations. The reports to support the success specifically in the field of food microbiology have been explained in the subsequent sections.

4 | HSI FOR DETECTION OF BACTERIA IN FOOD

4.1 | HSI to detect nonspore-forming bacteria in food

Bacteria can be classified based on several characteristics as Gram-positive or Gram-negative, aerobic and anaerobic, thermophiles, psychrophiles, mesophiles, motile and non-motile, and so forth. However, a major feature to classify bacteria as either resistant or non-resistant to cleaning and processing regimes is their classification as spore-forming and nonspore-forming bacteria. Those bacteria that do not form a dormant structure called a spore as a result of any stress and are comparatively more vulnerable to any heat or cleaning regime can be classified as "non-spore-forming." The use of HSI in the detection of nonspore-forming bacteria is listed in Table 4.

4.2 | HSI to detect spore-forming bacteria in food

Spore-forming bacteria impose a layer of challenge in detection and elimination due to their dormant nature, which makes them resistant to external stress (pH, nutrient limitations, desiccation, and temperature) (Soni et al., 2016). Bacterial spores can germinate into vegetative cells in the presence of favorable conditions such as nutrients (amino acids) or mild heat. For estimation of the presence or quantification of spores, culture-based methods rely on the germination of spores on media plates. An additional challenge is the presence of super dormant spores in food, which can be defined as the subpopulation that fails to germinate or germinate extremely slowly (Zhang & Mathys, 2019). Therefore, rapid nondestructive technologies, which do not rely on the germination of these spores, might be very useful as part of control strategies. While the research on robust detection of spore-forming bacteria is relatively limited as compared to that of vegetative forms, few reports in the literature show promising applications of HSI. Soni et al. (2021) reported the use of deep learning classification frameworks namely one-dimensional convolutional neural networks (1D-CNN) and random forest (RF) model for the detection of *Clostridium sporogenes* spores in ready-to-eat mashed potato. The combination of HSI (547−1701 nm) and modeling was a successful approach to differentiating dead and live forms of spores with an overall accuracy of 90−94%. It was concluded that the presence of dead spores in the matrix might induce significant artifacts in the results, and therefore the detection would need replicates and confirmatory assays to avoid including dead spores as viable forms. Another study by Anderson et al. (2008) reported the successful application of HSI in the range of 400−720 nm to detect dead from live spores of *Bacillus megaterium* and *Bacillus subtilis* when the spores were inactivated using chlorine and peroxide as a part of standard decontamination procedures. The study by Anderson et al. (2008) also stated that the specific spectral signature differences among dead and live spores could be specifically attributed to direct changes in the coat. Both these studies indicate a potential application of HSI in the detection of super dormant spores in food-based matrices; however, this needs further research.

4.3 | Identification and differentiation among bacterial strains using HSI in the food matrix

Detection of bacterial contaminants on food in a laboratory under controlled conditions can be relatively less complicated than the real food samples where multiple strains coexist. A recent study investigated if HSI can use the spectral signatures of individual cells of strains to later compare and cross-validate their accuracy for identification (Michael et al., 2019). PCA and k-nearest neighbor (kNN) classification followed by cross-validation showed 100% accuracy in the identification of *Comebacker sakazakii*, *E. coli* (O104, O111, and O145), *Salmonella serovar* Montevideo, and *L. monocytogenes*, whereas *E.*

TABLE 4 Applications of HSI in the detection of bacteria (nonspore formers)

Bacterial name and food matrix	HSI set-up used	Wavelength used	Analysis/algorithms used	Results	References
Lactobacillus curvatus VZ22 and *Lactobacillus sakei* VZ35 inoculated in commercial sliced cooked ham (10^3 CFU/slice)	Hyperspectral scanner operating in the near infra-red region equipped with Fourier-transform near-infrared spectrophotometer	900 to 1700 nm	Multivariate principal component analysis (PCA)	PCA was not capable of efficiently detecting the presence of bacteria with the raw spectra. Extensive data analysis using SNV transformation, second derivative, and column mean-centering enabled detection of the contamination and further identification of the two strains present	(Foca et al., 2016)
Total viable count (TVC) in pork meat	Hyperspectral scanner with a spatial resolution of 1628 × 618 pixels using a line-scan spectrograph	430–960 nm	Synergy interval PLS (SI-PLS), Gray-level co-occurrence matrix (GLCM), PCA-based image analysis, and Back-Propagation Artificial Neural Network (BP-ANN)	SNV was used to remove slope variation and correct light scatter. A back-propagation artificial neural network (BP-ANN) was developed to accurately predict TVC in pork meat	(Huang et al., 2013)
Enterobacteriaceae on chicken fillets	Push broom HSI system operating in the range of 930–1660 nm	450 to 900 nm	Partial least squares regression (PLSR) models	PLSR models enabled successful prediction of Enterobacteriaceae loads on chicken fillets ($R^2 \geq 0.82$) and root mean squared errors (RMSEs) ≤0.47 log CFU/g	(Feng et al., 2013)

(Continues)

TABLE 4 (Continued)

Bacterial name and food matrix	HSI set-up used	Wavelength used	Analysis/algorithms used	Results	References
Acidovorax citrulli on watermelon seeds	Raman HSI System	742.8 nm to 1014.2 nm	Polynomial fitting method was used along with F-values from the analysis of variance (ANOVA)	Successful detection of infected seeds from noninfected ones	(H. Lee et al., 2017)
E. coli, L. monocytogenes, S. aureus, S. Enteritidis, and *S. typhimurium*	Visible-near-infrared (VNIR) HSI system	700 to 900 nm	PCA, SVM, and linear discriminant analysis (LDA)	Identification of five strains from each other was possible in the peaks obtained in the range 700−900 nm, which correlated to the difference in the lipid fingerprints using modeling based on SVM and LDA	(Bonah et al., 2020)
Total bacterial counts in flounder fillets	Near infra-red (NIR) spectrometer was used to scan 6 points per fillet	600 to 1100 nm	PLSR, a combination of genetic algorithm (GA) and back-propagation artificial neural network (BP-ANN)	Successful detection of aerobic bacterial contaminants in the range of 3.7 log CFU/g to 9.8 log CFU/g, with increased efficiency and accuracy using GA and back-propagational artificial neural network (BP-ANN) model as compared to PLS model	(Duan et al., 2014)
E. coli on grass carp fish	HSI using line scanning	400 to 1000 nm	PLSR and multiple linear regression (MLR)	Quantification of *E. coli* ranging from 4 Log CFU/g to 10 Log CFU/g was successful	(Cheng & Sun, 2015)

TABLE 5 Applications of HSI in the detection of viruses

Name of the viral strain and food matrix	HSI set-up used	Wavelength used	Analysis/algorithms used	Results	References
Tomato spotted wilt virus (TSWV) in tobacco	Hyperspectral push broom spectral camera with halogen lamps for illumination	400–1000 nm	Successive projections algorithm (SPA) for wavelength selection and machine learning by boosted regression tree (BRT)	Overall accuracy of 85.2% in the detection of tomato spotted wilt virus (TSWV) infection in tobacco at an early stage (1–4 days of infection)	(Gu et al., 2019)
TSWV in plants of sweet pepper	Hyperspectral camera mounted on a Motorman robotic manipulator with halogen lamps for illumination	400–1000 nm	Maximum variance principal component analysis (MVPCA) and proximal sensing method-outlier removal auxiliary classifier generative adversarial nets (OR-AC-GAN)	Detection of infected plants was possible with an accuracy of 96.25% before visible symptoms were detected on the plants	(Wang et al., 2019)
Grapevine vein-clearing virus (GVCV) in grapevine plants	Push broom handheld hyperspectral camera used under natural light in the field	400—1000 nm	CNN (2-D and 3-D) modeling	Detection with 71% and 75% accuracy values was observed with 2D-CNN and 3D-CNN models, respectively.	(Nguyen et al., 2021)
Potato virus Y in seed potatoes	Line scan camera	400—1000 nm	Fully convolutional neural network (FCN)	Accuracy levels of 92% in the detection of the infected crop were achieved	(Polder et al., 2019)
Grapevine leafroll-associated virus 3 (GLRaV-3) in grapevine plants	Remote sensing using HSI	400–1000 nm	CART (Classification and Regression Tree) algorithm	Detection sensitivity averaged 94.1% (ranging from 88% to 99% per vineyard)	(MacDonald et al., 2016)

TABLE 6 Applications of HSI in the detection of fecal contamination in food

Food matrix	HSI set-up used	Wavelength used	Analysis/algorithms used	Results	Reference
Apple	HSI line scanning system for both reflectance and fluorescence measurements	400–900 nm	Two-band ratios, second differences, normalized differences, and absorption depth images	The fluorescence technique could differentiate normal apple surfaces from contaminated regions irrespective of apple skin coloration and manure thickness. Only thick patches of manure from the normal apple region could be detected with the reflectance method.	(Kim et al., 2001)
Apple	A multispectral laser-induced fluorescence imaging system with a light source (10 Hz optical parametric oscillator pulsed laser), A Gen II intensified charge-coupled-device (ICCD) camera with a common-aperture multispectral adaptor with a different interference filter was used for each quadrant used	400–900 nm	PC-based image processing/analyses software in MS Windows	The best results in the detection of feces were observed with fluorescence emission bands at 670 nm but multispectral fusion methods with band ratio image of 670 nm to 450 nm or 550 nm improved the sensitivity of detection.	(Kim et al., 2005)
Cantaloupe and strawberry	HSI line scanning system was used for reflectance and steady-state fluorescence measurements	425.7–951.2 nm	Two-band ratio and PCA-based image analysis	Specific bands were identified for developing multispectral fecal detection algorithms. Fecal contamination on best distinguished by the ratio of fluorescence emissions at 680 nm:745 nm and 660 nm for strawberries and cantaloupes, respectively.	(Vargas et al., 2004)

(Continues)

TABLE 6 (Continued)

Food matrix	HSI set-up used	Wavelength used	Analysis/algorithms used	Results	Reference
Lettuce and Spinach	An HSI line-scan imaging system with an electron-multiplying-charge-coupled device (EMCCD) camera, an imaging spectrograph, lenses, and a pair of ultraviolet (UV)-A lights at 365 nm	421–700 nm	Correlation coefficient and two-band ratio	The ratio of fluorescence intensities from two wavebands (666 nm and 680 nm) was used for the detection of bovine fecal contamination. The final binary images could successfully detect all fecal contamination spots on the adaxial and abaxial surfaces of romaine lettuce and baby spinach.	(Yang et al., 2010)
Chicken carcass	A digital camera with an outfitted prism-grating	465–823.5 nm	PCA	Results showed that fecal contamination could be visualized on artificially inoculated chicken carcass using PCA. This preliminary study concluded that larger sample size is required to ensure accurate measurements.	
Chicken carcass	A line-scan HSI system working the wavelength range of 430–900 nm.	400–900 nm	PCA	The ratio of images (565 nm:517 nm) was successfully used to identify fecal and ingesta contamination on the chicken carcass.	(Lawrence et al., 2001)

coli O45 and *Salmonella* Tennessee were not classified in the right group. This study also indicated that specific sublethal treatment could alter the spectral signature generated by the otherwise healthy strains. Specifically, lauric arginate treatment significantly altered the hyperspectral reflectance pattern generated by *C. sakazakii* BAA-894, *E. coli* O157, *S.* serovar Senftenberg, *L. monocytogenes*, and *S. aureus* cells (Michael et al., 2019). This alteration in the spectral signature could be attributed to the change in the physicochemical composition of the bacterial cells due to the chemical treatment. While this also indicated the sensitivity of HSI to discriminate between healthy and damaged cells, it highlights a significant challenge when the identification of strain in a large population is the objective. Extensive work is required to investigate the applicability of different classification models and validation techniques, which can eliminate the experimental errors and noise leading to poor classification.

5 | HSI TO DETECT FOODBORNE FUNGI

As outlined in Table 2, fungal contamination of food, especially fruits, vegetables, and cereals is common. Therefore, early and fast detection of fungi using novel techniques could contribute to a preventive strategy. Several studies demonstrate the detection of fungal contaminants in food using HSI when combined with chemometrics and machine learning. A near-infrared HSI system in the range of 400–1000 nm was used to classify maize kernels as infected or uninfected (Del Fiore et al., 2010). The spectra generated by *Rhizopus* spp., *A. niger*, *Fusarium* spp., and *A. flavus* present on maize (natural contamination) showed similarity to those obtained from pure cultures of these strains. Based on these preliminary results of the inoculation trials, it was concluded that HSI can discriminate commercial maize kernels infected with toxigenic fungi from uninfected controls within 48 h after the initial contamination of *A. niger* or *A. flavus* (Del Fiore et al., 2010). These outcomes were supported by a study by Chu et al. (2020) where HSI (900−1700 nm) was successful in the classification of maize kernels infected with fungi. Infection by *Fusarium* spp. can cause significant changes in quality-based attributes in wheat, rye, barley, and oats and has the potential to produce mycotoxins, which are known to cause poisonous and harmful effects in humans and animals (McCormick, 2003). A study by Bauriegel et al. (2011) indicated that HSI (400−1000 nm) can be successfully used to detect *Fusarium* infection in wheat in the early development stages before the morphological changes could become evident. The spectral changes detected were based on variations in the content of carotenoids (500−533 nm),

TABLE 7 Applications of HSI in the detection of foreign materials in food

Foreign material and food matrix	HSI set-up used	Wavelength used	Analysis/algorithms used	Results	Reference
Bones in chicken breast fillets	An HSI system with back-illuminated structured lighting	400–1000 nm	Illumination-transmittance model	Transmittance spectra of embedded bones were detected but could not be differentiated from nonbone scattering features (fat, connective tissue). Importantly, the bones embedded in compressed (thickness of 1 cm) samples were always detectable when the multimodes of imaging were fused in the final decision making.	
Plant parts in blueberries	A spectral imaging system with a stereoscopic microscope, a liquid crystal tunable filter (LCTF), and a monochrome CCD camera and wavelength of light transmitted through LCTF	400–720 nm	Spectral differences and thresholding	Plant organs contaminated with raw blueberry materials could be detected using spectral data and various thresholding techniques	
Leaves and stem parts in frozen blueberries	An imaging system with a NIR camera, a monochromator, and a NIR illuminator (400–1600 nm), where the camera was set up over the microscope	1000–1600 nm	Discriminant analysis	Successful visualization and detection of foreign materials of the same color dispersed in blueberries were accomplished by NIR spectral imaging using absorbance images at two wavelengths and discriminant analysis	

(Continues)

TABLE 7 (Continued)

Foreign material and food matrix	HSI set-up used	Wavelength used	Analysis/algorithms used	Results	Reference
Black walnut shell from pulp	A line-scan HSI system consisting of three modules (sensor, optics and lighting, and sample modules) and fluorescence imaging	425–775 nm	Gaussian-kernel based SVM, PCA, and Fisher's discriminant analysis (FDA) methods	Results indicated an overall recognition rate of 90.3% with the SVM approach for classifying walnut shells and pulp using hyperspectral fluorescence imagery	
Insect fragments in semolina	HSI system with two VariSpec LCTFs	900–1700 nm	PLSR	A positive correlation was found between three methods (manual, electronic speck counter, and HIS)	(Bhuvaneswari et al., 2011)
Polymer, wood, and metal particles on the surface of fresh raw broiler breast fillets	HSI	Visible-near infrared (VNIR) range (400–1000 nm) and the short-wave infrared (SWIR) range of 1000–2500 nm	PCA-based Mahalanobis distance (MD) metric model (PCA-MD), PLSR, and spectral angle mapper (SAM)	Fusion model successfully detected smaller (2×2 mm^2) pieces of polymer, wood, and metal with accuracies of 95%, 95%, and 81%, respectively, while the detection accuracies of the Fusion model for detecting larger (5×5 mm^2) pieces of polymer, wood, and metal were all 100%	(Chung & Yoon, 2021)
Bone fragments embedded in meat	A push broom-based short-wave near-infrared (SWIR) hyperspectral reflectance imaging system	1000–1700 nm	PCA and Image subtraction	Detection accuracy of 93.3% and wavelength of 1153.8-nm (53rd band) indicated a strong reflection intensity in the average spectrum of bone fragments embedded in the chicken breast fillets)	(Lim et al., 2020)

TABLE 8 Applications of HSI in the detection of chemical contaminants in food

Food matrix and contaminant	HSI set-up used	Wavelength used	Analysis/algorithms used	Results	References
Melamine in wheat flour	A wide-field NIR chemical imaging system	1000–1650 nm	PLSR	PLSR model built from NIR imaging data showed a correlation to the melamine concentration, yielding a SEP of 0.6%. The limit of quantification (LOQ) was attributed to a small training set (24) of spectra over the full melamine concentration range.	(Priore et al., 2009)
Pesticide (dichlorvos residue) in navel oranges	A line-scan HSI system	400–1000 nm	PLSR	Two PLS models were built from the HSI data and GC reference data of dichlorvos residue, where the first model had a full spectral range and the second had 20 optimal wavelengths. The second model showed lower performance in terms of PLS statistics.	(J. Li et al., 2010)
Pesticide (methamidophos) in spinach leaf	A hyperspectral fluorescence with a microscope, LCTF, a monochrome CCD camera, and a spectral illuminator (200–1000 nm).	400 to 720 nm	LDA and SVM	The hyperspectral excitation-emission matrix (EEM) data were effective in the detection of methamidophos on spinach leaves. In the pixel-wise validation, the misclassification ratio for SVM was 0.099 while that for LDA was 0.188. SVM also showed better results than LDA as the misclassification ratios for SVM and LDA were 0.092 and 0.162, respectively.	(Tsuta et al., 2009)

chlorophylls (560−675 nm and 682−733 nm), and water content in the tissues (927−931 nm) (Bauriegel et al., 2011). As compared to the healthy wheat ears, a decrease in the absorption in the range of the chlorophyll bands were observed in the *Fusarium*-infected tissues. This was postulated to be the result of the destruction of chloroplasts and degradation of chlorophylls (Bauriegel et al., 2011; Kang & Buchenauer, 2000). Similar changes in the spectral bands of chlorophylls were also detected in infected tissues alongside the spectral variations in the range of 927−931 nm, which was indicative of the water loss in the undetected tissues (Bauriegel et al., 2011). In this study, a new classification method was created and named head blight index (HBI) which was based on the difference in reflectance between the starting point (550−560 nm) and the endpoint (665−675 nm) to differentiate the healthy ears from infected ones and to reduce the background noise. Similarly, wheat grain infections have been able to be characterized using NIR-HSI (1000−1600 nm), and the difference in the spectral signatures based on the strains has been evaluated. This study reported an accuracy of 92.9%, 87.2%, 99.3%, and 100% for wheat kernels infected by *A. niger*, *A. glaucus*, *Penicillium* spp., and healthy wheat kernels, respectively, using statistical analysis with PCA and multiclass support vector machine with radial basis function (H. Zhang et al., 2007). Fungal infections on grains were detectable by HSI at a very early level indicating potential early detection for removal of the infected parts to eliminate or reduce the spread of fungal infections.

6 | HSI TO DETECT FOODBORNE VIRUSES

Viruses cannot replicate and reproduce in food as they need living cells to replicate; however, food matrices are well established as vehicles for the transmission of infectious pathogens (Petrović & D'Agostino, 2016). Reliable and accurate identification of viruses is vastly dependent on their ability to colonize plant or animal cell lines. HSI is at an early stage where the structural and morphological features of either the structural components of the viruses (nucleic acid, protein coat, or capsid particles) or the infected parts of the plants can be used to derive a spatial signature, and the data are then reduced in dimension using multivariate analysis. The studies reported so far with HSI as a tool to detect viruses or virus-infected plants are summarized in Table 5.

Validation of HSI as a tool to detect and identify viruses in food matrices, especially in the presence of a mixed microbial population remains underreported. This could be attributed to several factors including the size of the viruses, the high level of sensitivity required, and limited and expensive alternative methods to confirm the presence as part of any standardization protocol.

7 | HSI AS A DETECTION TOOL FOR PHYSICAL CONTAMINANTS IN FOOD

HSI has been used in the Vis-NIR (400–1000 nm) or NIR (1000–1700 nm) range to detect contaminants in fruits, vegetables, and meat products (Gowen et al., 2007). The feasibility of this technology combining the spatial and spectral information to detect defects and properties related to the composition of meat products has been reported (Al-Sarayreh et al., 2019; Díaz et al., 2011). The two main issues related to the physical contamination of food are fecal contamination and the presence of foreign materials in food matrices (Feng & Sun, 2012). Contamination due to fecal ingesta can introduce pathogenic microorganisms in fruits, vegetables, and meat, which could potentially cause food poisoning (Feng & Sun, 2012). Therefore, fecal contamination is considered a food safety concern due to its association with various fungal and bacterial contaminants. Table 6 illustrates various studies conducted using HSI for the detection of faucal contamination in fruits, vegetables, and poultry meat. HSI in the detection of foreign material acts as a robust detection tool in quality control in food processing and packaging facilities (Table 7). The presence of foreign particles can be a route to potential transmission of pathogens in the food processing environment (Kusumaningrum et al., 2003), and therefore the detection of foreign particles would not only be a barrier to consumer acceptance but is also a concern to food safety and shelf life.

8 | HSI AS A DETECTION TOOL FOR CHEMICAL CONTAMINANTS IN FOOD

Chemical contamination detection by HSI involves only limited studies (Table 8). Two main categories are being discussed, namely melamine and pesticide residue. Melamine has been a big food safety-related concern, especially due to the outbreak of the milk powder scandal in 2008 in China (Y.-N. Wu et al., 2009). Melamine is used in the manufacture of laminates, coatings, dishware, kitchenware, and also as a flame retardant when mixed with resins (Q. Li et al., 2019). The harmful effect of melamine on humans and animals are many including pediatric nephrolithiasis, nephrotoxicity, and acute kidney injury with the formation of kidney stones being the most common clinical manifestation (Q. Li et al., 2019; Sharma & Paradakar, 2010). Table 8 discusses the studies where HSI was used to detect melamine. Another major issue is

the accumulation of pesticide residue in the human body due to the consumption of contaminated food. This could lead to chronic diseases, such as cancer, diabetes, and so forth (Bolognesi & Morasso, 2000). Table 8 discusses the studies focused on detecting pesticide residues via the HSI technique.

9 | INTERPRETATION OF SUITABLE ALGORITHMS AND CHEMOMETRICS FOR OPTIMIZED RESULTS

Interpreting the HSI data for identifying species of interest (e.g., microbes, contaminant, etc.) require the use of chemometric-based algorithms. Tables 4–8 illustrate various techniques that have been used for identifying microorganisms, food contaminants, fecal material, or chemicals in food. Interpretation of the chemometrics involved plays a major role in the final prediction or results. For example, Foca et al. (2016) used PCA for detecting LAB in a Petri dish and sliced ham. Preprocessing with a combination of detrending and column mean-centering allowed the best discrimination for background and Petri dish. Further, PC2 allowed the distinction of two different bacterial strains. This separation could be attributed to preprocessing, which eliminated any background effects and thus enhanced the relevant spectral bands contributing to the detection of the two microbial species with PCA (Foca et al., 2016). Since PCA loadings were not provided in the study, relevant wavelengths could not be interpreted.

In another study (Table 5), related to virus detection, Gu et al. (2019) used three wavelength selection methods and four ML techniques for detecting TSWV infection in tobacco. BRT-SPA model showed the best performance. The BRT method selected the highest number of wavelengths (8 vs. 6) and probably captured wavelengths most related to TSWV. Furthermore, SPA removed any redundant information, which was then successfully used to discriminate between diseased and healthy tobacco. In a study by Yang et al. (2010) related to fecal contamination detection in green leafy vegetables (Table 6), correlation analysis was used to determine optimal wavebands, whose ratio images were then used for the detection of fecal contamination spots on lettuce and spinach leaves. For both products, the coefficient (~1) was obtained from the ratio of the wavebands 666 nm and 680 nm. The main reason for the selection of these fluorescence intensities (666 nm and 680 nm) was their correspondence to fluorescence emission peaks for fecal matter and chlorophyll (Yang et al., 2010). Leafy green vegetables have relatively higher chlorophyll as compared to fecal contamination spots. The ratio of fluorescence intensities showed better results than the single intensity images for fecal contamination detection. Tsuta et al. (2006) used second derivative preprocessing for enhancing any overlapping peaks capable of detecting foreign material in blueberries and also to remove any baseline shifts from the spectra, which could otherwise produce artifacts (Table 7). The second derivative spectra of foreign matter (plant organs) showed a negative peak at 680 nm, which was detected by processing the second derivative absorbance image at this wavelength and was considered to be derived from the absorption band of chlorophyll.

For detecting melamine in wheat flour (Table 8), Priore et al. (2009) used PLSR to build a model in which the most intensive peak that provided a significant difference was found to be at 1468 nm, which was related to NH asymmetric stretching (Tang et al., 2016). The peak was enhanced via first derivative preprocessing and was then utilized by PLSR to build the model. However, the limit of quantification (LOQ) was restricted by the availability of only 24 spectra. Explanation of chemometrics used for all the studies in Table 4–8 warrants for a separate review focused on chemometrics for detecting microbes and food contaminants via HSI.

10 | CHALLENGES AND MITIGATION STRATEGIES FOR HSI-BASED DETECTION

Hyperspectral data consists of a three-dimensional data cube made up of vector pixels (voxels). These vector pixels are made up of spectral information as well as 2D spatial information (Wu & Sun, 2013). Each spatial point is extracted into a spectrum with a general spatial sampling rate (e.g., 10 points in 1 mm), which results in image cubes that can be thousands of gigabytes (Cucci & Casini, 2020). Therefore, the data obtained do not only consist of relevant information about specific compounds but is also made up of a huge amount of nonspecific background information. For example, random/systematic noise, variations based on the chemical or physical nature of the matrix due to physical, chemical, and structural disorientations. The information obtained can also vary based on the technique and the equipment used for image acquisition as well as external factors such as environmental conditions (Amigo & Santos, 2019). The structural components of the food matrix can also affect the light interaction with samples generating a spectral signal that overlaps with the spectral signal of microorganisms present. The ability of HSI to collect spatial and spectral information creates the possibility to mitigate the effect of the matrix but it requires the use of methods that can process these two types of information (Jia et al., 2020; Vidal & Amigo, 2012). The following

section reviews approaches that have been used to address these challenges.

10.1 | Background-based interference

The spectral signals associated with the components of the food matrices might severely interfere with the detection of microorganisms in food. For example, a study by Foca et al. (2016) investigated the use of HSI and spectral techniques to detect lactic acid bacteria (LAB). The two species of *L. sakei* and *L. curvatus* on De Man, Rogosa, and Sharpe (MRS) plates were distinguishable using PCA constructed using the spectral variables between 955 nm and 1700 nm. However, a similar result could not be obtained using hyperspectrograms obtained from the segmented images of inoculated ham. This was postulated to be due to more than one reason. For example, a thin deposition of the bacterial cells (when 10^8 CFU/ml) on the flat surface of the ham might have led to overdilution of the LAB, which could be below the detection limit. Another postulated reason was the overcomplexity and therefore contribution of the rich background matrix (ham) onto the spectra, which led to over masking the bacterial signatures.

Huang et al. (2013) attempted to estimate TVC on pork meat and the results indicated the presence of artifacts due to the complexity of the matrix. A linear relationship could not be established between the hyperspectral data cube (generated using a quadrate region of interest [ROI] [200 × 200 pixels] selected in the spatial range of 450−900 nm) and the bacterial numbers in pork meat and the characteristic indicators of spoilage. However, BP-ANN model was generated using data fusion, which resulted in a prediction accuracy of 83% in the determination of TVC during the spoilage process (Figure 2). Microbiological spoilage is associated with two main aspects: an increase in the total bacterial numbers in the pork meat and a reduction in pork freshness due to the gradual increase in biochemical reactions by these bacteria during storage. The biochemical changes can further be classified as enzyme-catalyzed breakdown of carbohydrates, protein, and fat, thereby producing byproducts such as ketones, ammonia, hydrogen sulfide, alcohols, carboxylic acid, and gases (Huang et al., 2013). All these biochemicals could be directly linked to the spoilage of pork meat. This study attempted a TVC prediction model using BP-ANN by data fusion through seven PCs from spectra and four PCs from images. This model (Figure 2c) based on data fusion used the external and internal attributes in pork meat, therefore, was more accurate in predicting the bacterial count as compared to the other two models (model based on image [Figure 2a] and model based on spectra [Figure 2b]).

The model using data fusion by Huang et al. (2013) which integrated spectral and image information indicated significant potential in the determination of TVC in pork meat as compared to the model that uses either spectral or image-based information. HSI poses a specific challenge of differentiation among the strains on complex food surfaces. A study by Bonah et al. (2020) reported the use of wavelength selection using specific wavebands that represent lipid fingerprints generated by the differences in structure and composition of the cell wall and cell membranes as a useful tool for differentiation among strains. For example, absorption (700–900 nm) of hydrogen-bearing groups (CH, OH, and NH) could be correlated with lipids, which are commonly found in bacterial cell walls (Alexandrakis et al. 2008; Bonah et al., 2020). These molecules are abundant in living cells, and although there is a variety of possible combinations of different acyl arms and head groups, lipids could be linked back to specific species. Simplified models based on such fingerprints can be further used for generating models using partial least-squares discriminant analysis (PLS-DA), and soft independent modelling of class analogy (SIMCA) (Alexandrakis et al., 2008) can be used to further increase the classification efficacy. In the study by Bonah et al. (2020), a model named CARS-PSO-SVM, which was a combination of competitive adaptive weighted sampling or CARS (for wavelength selection), particle swarm optimization or PSO (for classification-training and prediction) and support vector machine or SVM (for parameter optimization) was successful in the classification of foodborne pathogens on agar plates. This work indicated that the background interference could be reduced by combining HSI with chemometric techniques.

10.2 | Limit of detection

The studies evaluating the efficiency of HSI in the quantification of bacterial load in food samples are very limited. A study by Cheng and Sun (2015) investigated the potential and suitability of HSI (400−1000 nm) for the detection and quantification of *E. coli* in fresh grass carps (flesh) during the spoilage process while being stored at 4°C (Cheng & Sun, 2015). The results indicated that the spectral preprocessing method of multiplicative scatter correction (MSC) combined with multivariate analysis using PLSR model showed a good performance in predicting a change up to 0.3 log CFU/g (Cheng & Sun, 2015). However, the spectral signature itself could not indicate a major difference in the reflectance patterns among bacterial loads with a difference of up to 2 log CFU/g, indicating that preprocessing and modeling were essential to increase the efficiency and sensitivity (Cheng & Sun, 2015). Also, bacterial spoilage

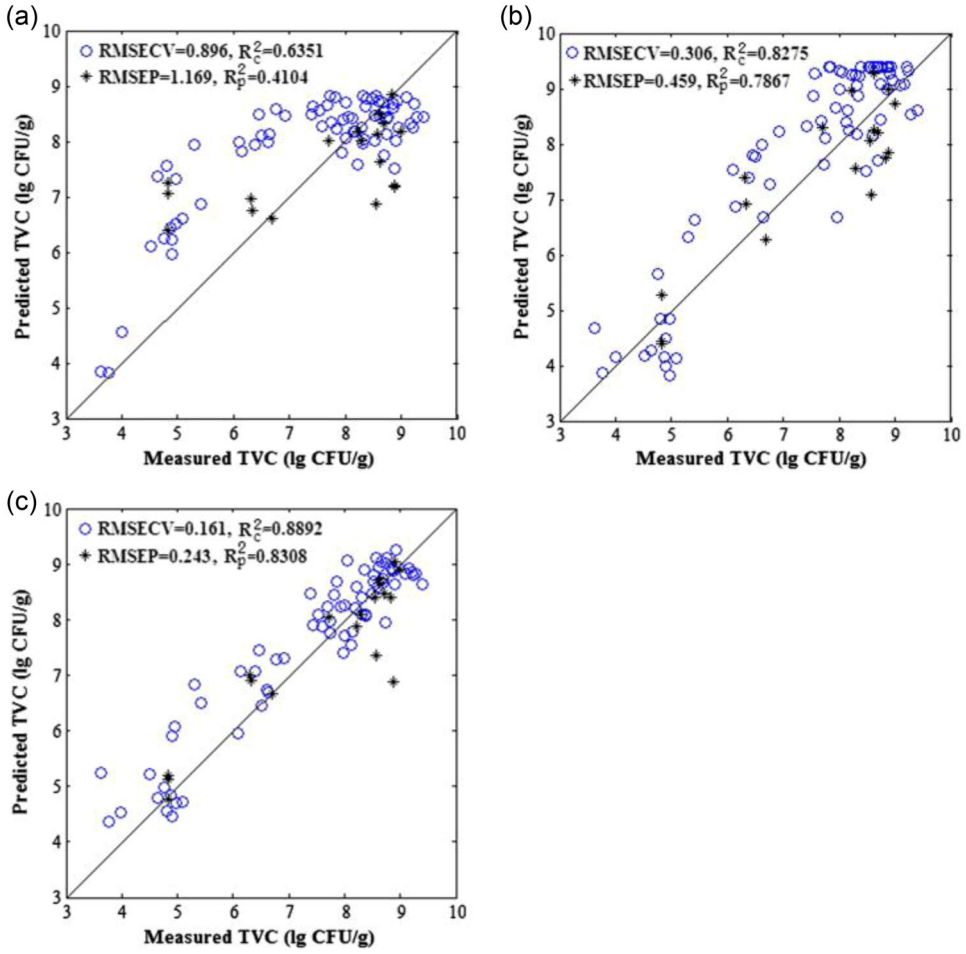

FIGURE 2 Scatter plots of three models between the prediction values and the reference measurement values. (a) Model based on the image; (b) model based on spectra; (c) model based on data fusion. Reprinted from rapid detection of total viable count (TVC) in pork meat by hyperspectral imaging. Huang et al. (2013) with permission from Elsevier (License number: 5281690473945)

over time was associated with a change in color intensity from blue to red, and this change was further associated with uneven distribution of nutrients and therefore uneven level of biochemical changes post spoilage. This was useful and necessary in generating a prediction image using modeling using MLR (Cheng & Sun, 2015). Another study that investigated the quantification ability of HSI targeted TVC rather than specific strains on meat (Huang et al., 2013). In this study, a model was developed based on data fusion using SNV to remove slope variation along with a BP-ANN. The results supported the conclusion by Cheng and Sun (2015), and the limit of detection was similar (0.2 log CFU/g) as compared to the reflectance itself, which could differentiate spoilt meat from controls but could not estimate the bacterial load and the inefficiency increased with increase in bacterial load (Huang et al., 2013). The studies by Cheng and Sun (2015) and Huang et al. (2013) indicated that although lower numbers of bacterial loads could be difficult to detect, there are biochemical changes at an early stage of the onset of spoilage, which could not be detected by human eyesight, but could be detected using HSI and modeling approaches and could be indirectly linked to bacterial load for prediction. In another study by Soni et al. (2021), where the concentration of *C. sporogenes* spores was successfully predicted using CNN as well as RF model with a limit of detection of up to 10 CFU/ml, while dead spores were included in the analyzed samples. This study indicated that modeling can significantly improve the efficiency of HSI in differentiating live from the dead population of bacteria and can be used to detect the surviving (viable) spores after any lethal treatment (Soni et al., 2021). Therefore, the bacterial load could be quantified in food models, provided the data extraction is combined with a modeling approach to reduce the effect of background by employing deep learning models like CNN networks.

10.3 | Risks associated with the lack of identification in a diverse population

TVC of bacteria in food products is routinely determined by food industries as a part of predicting spoilage as well as shelf life. This also helps to check the acceptable limits above which the risk of health problems owing to the generation of toxic compounds in the food is indicated. However, it is not only essential to determine the TVC but also to determine the strains present in the sample being tested, especially because there are many strains that even if present in extremely low concentration (1 cell/sample), would lead to food poisoning. Such examples include *L. monocytogenes*, for which there is a "zero-tolerance" policy in some countries (Bover-Cid et al., 2011). For such strains of importance, the use of HSI as a tool for detection poses a risk where the specific strains of importance would not be differentiated from the rest of the population, especially if the proportion of the target population is low. Further research on complex matrices including background microbial flora and various microbial strains to allow better the identification, specificity, and lower detection limits would increase the potential applications of HSI.

11 | USING MACHINE LEARNING IN COMBINATION WITH HSI AS A MITIGATION STRATEGY

While there are many advantages of using HSI over conventional methods for rapid, nondestructive, and lateral assays, there are a few challenges such as the heterogeneous nature of the food matrix, presence of multiple levels of populations in samples and inconsistency in the chemical attributes of real samples, unlike food models. Complex chemometric approaches and artificial intelligence-based technologies are used extensively to model and extract the information from data obtained using HSI. Machine learning methods can be broadly divided into three types namely, supervised machine learning, unsupervised machine learning, and reinforced machine learning (Misra et al., 2022; Ozdemir & Polat, 2020). Supervised machine learning can be explained as a method that utilizes a ground truth to extract information from spectral data. Examples of supervised machine learning are SVM, k-Nearest Neighborhood (KNN), Decision Trees, Random Forest, Linear Regression, and Neural Networks (NN) (Ozdemir & Polat, 2020; Urbanos et al., 2021). As explained in various sections of this review, the use of machine learning and chemometrics can enhance the detection efficiency and reduce the background noise to employ HSI as a routine detection method. For example, the study by Soni et al. (2021) used deep learning classification frameworks namely 1D CNN and RF to detect and quantify *C. sporogenes* spores in a complex food matrix of mashed potato. This study also indicated the efficiency of modeling in discriminating between the dead and live spores and resulted in an overall accuracy of 90–94% (Figure 3) when the dead/inactivated spores were present and absent, respectively (Soni et al., 2021).

Therefore, this study developed a method to overcome the nonlinearity introduced by the signal of the food matrix and successfully detect the useful information that helped in differentiating dead and live spores. A study by Park et al. (2012) successfully developed a protocol for immobilizing live-cell on glass slides to acquire spectral images from serotypes of Shiga-toxin producing *E. coli* (STEC), namely O26:H2, strain 4; O45:H2, strain 8; O103:H2, strain D; O111:H1, strain 16; O121:H19, strain A; and O145:H-, strain K. In this study, 100 samples of six different STEC serotypes were used for testing two algorithms (SVM and Sparse Kernel-based Ensemble Learning [SKEL]), and the samples were selected from cells at a pixel level. Serotype O45 was classified with 92% detection accuracy using both the algorithms tested. However, for all the other serotypes, the accuracies were found to be 68.3% and 68.1% for SVM and SKEL, respectively (Park et al., 2012). Although no specific reason was reported for the low accuracies, it was postulated that minimizing sample variability and optimizing parameter selection of the system such as consistency in light exposure would be useful.

PCA and multiclass SVM and Soft Robust Independent Modelling of Class Analogies (RSIMCA) has also shown precision (P) and recall (R) value of more than 95 and 98%, respectively when used for detection of bacteria causing urinary tract infection (urinary tract infection [UTI] bacteria [*E. coli*; *Enterococcus faecalis*; *S. aureus*; *Proteus mirabilis, Candida albicans* and *Proteus vulgaris*]) (Turra et al., 2015). Each pathogen tested showed an accuracy of greater than 95% and 98%, respectively, except for *C. albicans* where the spectral signature assessment due to the small size of colonies led to reduced spatial resolution. RSIMCA maximized the information of each class (micro), thereby distinguishing each class from the rest of the information including the background and significantly improved the performance on the same dataset. The ability to work with multiple pathogen-optimized feature spaces was improved, hence making the whole system highly flexible for the inclusion of additional pathogens. The study by Turra et al. (2015) successfully showed the implementation and testing of the HSI system for rapid acquisition and discrimination of bacterial causing urinary tract infections (UTI). The bacterial colonies on blood agar plates were again targeted for detection and analysis using 1-D CNN, SVM in an extended study

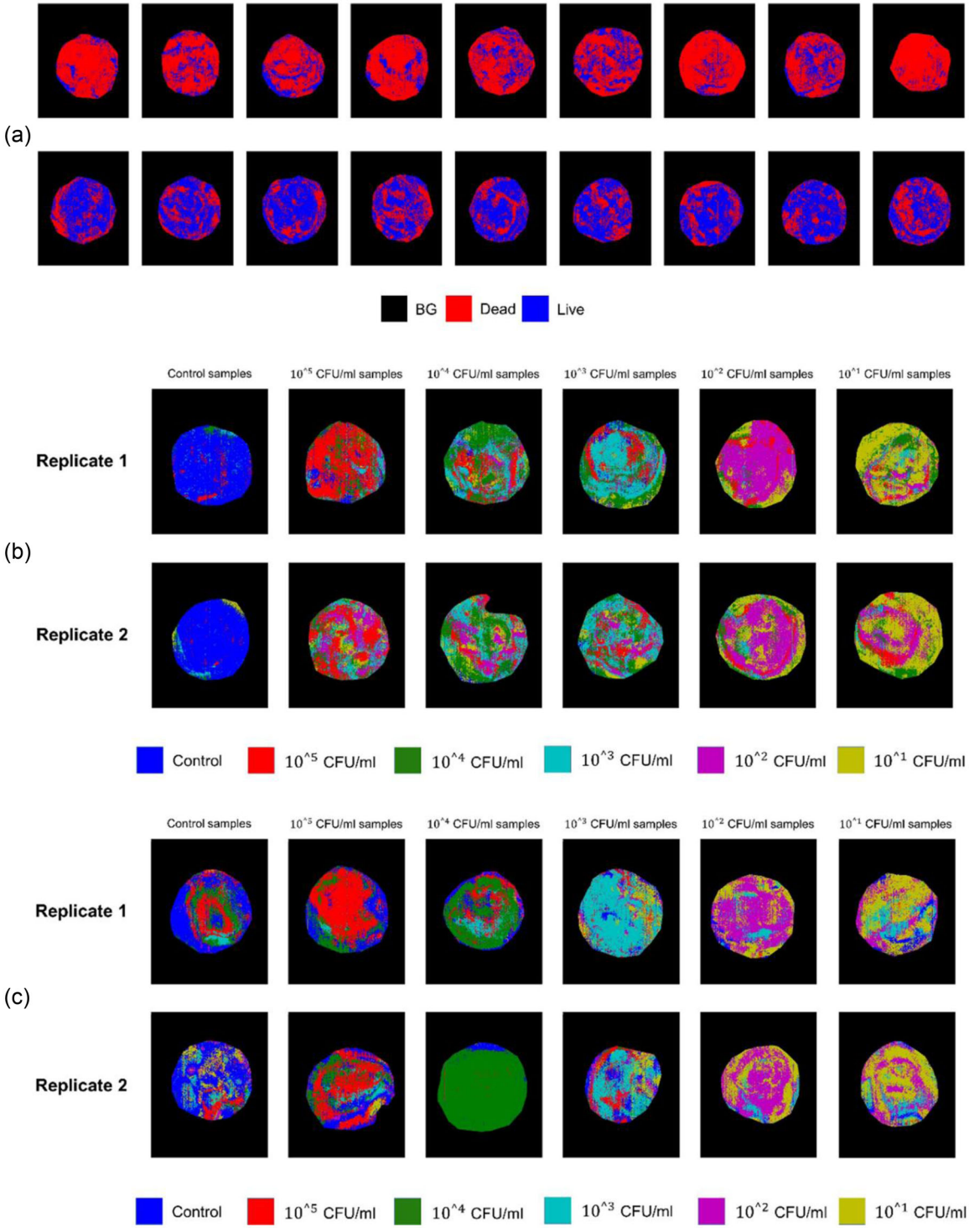

FIGURE 3 Classification of spores as dead and live using results from the CNN model. Classification maps of *C. sporogenes* spores based on physiological state (a), based on the inoculum levels on mashed potato when diluted in 0.1% peptone water (b), and based on their inoculum levels on mashed potato when diluted in dead/autoclaved spore suspension (c). Reprinted from Soni et al. (2021), with permission from Elsevier (License Number 5296880777912)

(Arrigoni et al., 2017). In the 1D CNN approach, instead of considering single-pixel spectra, the CNN sees the extracted colony spectral signatures (CSS) as inputs while producing the colony-based class scores as output alongside using SVM and RF for comparison purposes. According to the results, the CNN model was chosen as the best method, which yielded an accuracy of 99.7%. This study showed the potential of applying HSI in the VNIR spectrum and a deep learning approach such as CNN for analyzing the nonlinear effect of matrix on signal of microorganisms as in this case, for the identification of bacteria causing UTI (Arrigoni et al., 2017).

Another study compared the efficiency of seven machine learning methods (ordinary least squares regression [OLS-R], stepwise linear regression [SL-R], principal component regression [PC-R], PLSR, Support Vector Machines Regression [SVM-R], Random Forests Regression [RF-R], and k-Nearest Neighbours' Regression [kNN-R]) to predict bacterial counts for TVC, LAB, Pseudomonads, Enterobacteriaceae, and *B. thermosphacta* in minced beef (Estelles-Lopez et al., 2017). All seven methods were evaluated for their performance, using RMSE as a measure for the model's performance validation. Under aerobic conditions, MSI generated the best results for Pseudomonads with PLSR. Under modified atmosphere packaging (MAP), MSI showed good prediction accuracy for *Lactobacilli* and *B. thermosphacta*, both using RF-R (Estelles-Lopez et al., 2017). Additionally, in this study, an interactive online platform "MeatReg" was developed to determine the most suitable regression ML method to generate the best prediction accuracy of different types of microorganisms involved in beef spoilage using data from five different analytical methods (Estelles-Lopez et al., 2017).

12 | CONCLUSION AND FUTURE PERSPECTIVES

The application of HSI for the detection of bacteria, fungi, and viruses in food-based matrices, which are different and complex as compared to the model systems and media plates was reviewed. As HSI provides a plethora of information (spatial–spectral), it allows more complex models (e.g., CNN) to be used to deal with the complex interaction between the signal generated by the microbial cells and the food matrix. Although this area has not been extensively explored, some studies in this area have shown promising results. The use of HSI in the detection of bacteria, viruses, and fungi in food matrices, also extends to a potential application in the quantification of these microbes. Further research on the following areas would add significant potential to the use of HSI as a tool for the identification and detection of pathogens:

1. There is an evident research gap in the number of studies that have reported the use of HSI (and machine learning) to quantify viruses, fungi, and allergens as well as prions. Prions can lead to substantial, neurodegenerative disorders that affect both humans and animals. A study by Stepanchuk et al. (2021) has indicated success in the use of a combined approach with spectral imaging and amyloid probes for the early detection of tissues infected with prions. This approach could be extended to HIS to discover markers that could enable the early detection of prions in food.
2. The combination of HSI and microscopy indicates the capability to capture unique signals related to microorganisms regardless of their cell size. Also, the application of deep learning of HSI data helps to extract the underlying information and modeling approaches help to develop screening systems that could be incorporated into the routine analysis. This will only be possible when the detection limit of HSI would be as low as 1 cell/sample including identification of the bacterium, therefore warrants further research.
3. Determination of quality attributes of food that are due to the presence of spoilage-inducing microorganisms could be a potential area of research that would enable the prevention of recalls as well as food wastage.

With rapid developments and the creation of databases, HSI might be able to develop as a routine analytical method in food microbiology for industries and commercial labs.

ACKNOWLEDGMENTS

The research outlined in this study was supported by the AgResearch Ltd Strategic Science Investment Fund (A25768).

Open access publishing facilitated by AgResearch Ltd, as part of the Wiley.

AUTHOR CONTRIBUTIONS

Aswathi Soni: formal analysis; investigation; methodology; writing – original draft; writing – review & editing. **Yash Dixit**: resources; writing – original draft; writing – review & editing. **Gale Brightwell**: conceptualization; funding acquisition; writing – review & editing.

CONFLICT OF INTEREST

The authors declare no conflict of interest.

ORCID

Aswathi Soni https://orcid.org/0000-0002-8546-2858
Yash Dixit https://orcid.org/0000-0002-7913-8437
Marlon M. Reis https://orcid.org/0000-0003-1930-1316
Gale Brightwell https://orcid.org/0000-0002-3980-4108

REFERENCES

Abeywickrama, K., & Bean, G. A. (1991). Toxigenic *Aspergillus flavus* and aflatoxins in Sri Lankan medicinal plant material. *Mycopathologia*, *113*(3), 187–190.

Acheson, D., & Fiore, A. E. (2004). Hepatitis A transmitted by food. *Clinical Infectious Diseases*, *38*(5), 705–715.

Agriopoulou, S., Stamatelopoulou, E., & Varzakas, T. (2020). Advances in analysis and detection of major mycotoxins in foods. *Foods*, *9*(4), 518.

Akindolire, M. A., Babalola, O. O., & Ateba, C. N. (2015). Detection of antibiotic resistant *Staphylococcus aureus* from milk: A public health implication. *International Journal of Environmental Research and Public Health*, *12*(9), 10254–10275.

Al-Sarayreh, M., Reis, M. M., Yan, W. Q., & Klette, R. (2019), September 3–5. *A sequential CNN approach for foreign object detection in hyperspectral images* [Paper presentation]. The International Conference on Computer Analysis of Images and Patterns, Salerno, Italy.

Alexandrakis, D., Downey, G., & Scannell, A. G. M. (2008). Detection and identification of bacteria in an isolated system with near-infrared spectroscopy and multivariate analysis. *Journal of Agricultural and Food Chemistry*, *56*(10), 3431–3437. https://doi.org/10.1021/jf073407x

Alshannaq, A., & Yu, J.-H. (2017). Occurrence, toxicity, and analysis of major mycotoxins in food. *International Journal of Environmental Research and Public Health*, *14*(6), 632.

Amigo, J. M., & Santos, C. (2019). Chapter 2.1—Preprocessing of hyperspectral and multispectral images. In J. M. Amigo (Ed.), *Data handling in science and technology* (Vol., 32, pp. 37–53). Elsevier.

Anderson, J., Reynolds, C., Ringelberg, D., Edwards, J., & Foley, K. (2008). Differentiation of live-viable versus dead bacterial endospores by calibrated hyperspectral reflectance microscopy. *Journal of Microscopy*, *232*(1), 130–136.

Ang, B. S., Lim, T. C., & Wang, L. (2018). Nipah virus infection. *Journal of Clinical Microbiology*, *56*(6), e01875–01817.

Ankolekar, C., Rahmati, T., & Labbé, R. G. (2009). Detection of toxigenic *Bacillus cereus* and *Bacillus thuringiensis* spores in U.*S. rice*. *International Journal of Food Microbiology*, *128*(3), 460–466. https://doi.org/10.1016/j.ijfoodmicro.2008.10.006

Arefi, A., Sturm, B., von Gersdorff, G., Nasirahmadi, A., & Hensel, O. (2021). Vis-NIR hyperspectral imaging along with Gaussian process regression to monitor quality attributes of apple slices during drying. *LWT*, *152*, 112297.

Argudín, M. Á., Mendoza, M. C., & Rodicio, M. R. (2010). Food poisoning and *Staphylococcus aureus* enterotoxins. *Toxins*, *2*(7), 1751–1773. https://www.mdpi.com/2072-6651/2/7/1751

Armstrong, G. L., Hollingsworth, J., & Glenn, M. J. (1996). Emerging foodborne pathogens: *Escherichia coli* O157: H7 as a model of entry of a new pathogen into the food supply of the developed world. *Epidemiologic reviews*, *18*, 29–51. https://doi.org/10.1093/oxfordjournals.epirev.a017914

Arrigoni, S., Turra, G., & Signoroni, A. (2017). Hyperspectral image analysis for rapid and accurate discrimination of bacterial infections: A benchmark study. *Computers in Biology and Medicine*, *88*, 60–71. https://doi.org/10.1016/j.compbiomed.2017.06.018

Banerji, R., Karkee, A., Kanojiya, P., & Saroj, S. D. (2021). Pore-forming toxins of foodborne pathogens. *Comprehensive Reviews in Food Science and Food Safety*, *20*(3), 2265–2285.

Bauriegel, E., Giebel, A., Geyer, M., Schmidt, U., & Herppich, W. (2011). Early detection of *Fusarium* infection in wheat using hyperspectral imaging. *Computers and Electronics in Agriculture*, *75*(2), 304–312.

Benedict, K., Chiller, T. M., & Mody, R. K. (2016). Invasive fungal infections acquired from contaminated food or nutritional supplements: A review of the literature. *Foodborne Pathog Dis*, *13*(7), 343–349. https://doi.org/10.1089/fpd.2015.2108

Bennett, J. W., & Klich, M. (2003). Mycotoxins. *Clinical Microbiology Reviews*, *16*(3), 497–516. https://doi.org/10.1128/CMR.16.3.497-516.2003

Beuchat, L. R. (1996). *Listeria monocytogenes*: Incidence on vegetables. *Food Control*, *7*(4–5), 223–228.

Bhuvaneswari, K., Fields, P. G., White, N. D., Sarkar, A. K., Singh, C. B., & Jayas, D. S. (2011). Image analysis for detecting insect fragments in semolina. *Journal of Stored Products Research*, *47*(1), 20–24.

Bolognesi, C., & Morasso, G. (2000). Genotoxicity of pesticides: Potential risk for consumers. *Trends in Food Science & Technology*, *11*(4–5), 182–187.

Bonah, E., Huang, X., Yi, R., Aheto, J. H., & Yu, S. (2020). Vis-NIR hyperspectral imaging for the classification of bacterial foodborne pathogens based on pixel-wise analysis and a novel CARS-PSO-SVM model. *Infrared Physics & Technology*, *105*, 103220. https://doi.org/10.1016/j.infrared.2020.103220

Bosch, A., Gkogka, E., Le Guyader, F. S., Loisy-Hamon, F., Lee, A., van Lieshout, L., Marthi, B., Myrmel, M., Sansom, A., Schultz, A. C., Winkler, A., Zuber, S., & Phister, T. (2018). Foodborne viruses: Detection, risk assessment, and control options in food processing. *International Journal of Food Microbiology*, *285*, 110–128. https://doi.org/10.1016/j.ijfoodmicro.2018.06.001

Bosch, A., Sánchez, G., Abbaszadegan, M., Carducci, A., Guix, S., Le Guyader, F. S., Netshikweta, R., Pintó, R. M., van der Poel, W. H. M., Rutjes, S., Sano, D., Taylor, M. B., van Zyl, W. B., Rodríguez-Lázaro, D., Kovač, K., & Sellwood, J. (2011). Analytical methods for virus detection in water and food. *Food Analytical Methods*, *4*(1), 4–12. https://doi.org/10.1007/s12161-010-9161-5

Bover-Cid, S., Belletti, N., Garriga, M., & Aymerich, T. (2011). Model for *Listeria monocytogenes* inactivation on dry-cured ham by high hydrostatic pressure processing. *Food Microbiology*, *28*(4), 804–809. https://doi.org/10.1016/j.fm.2010.05.005

Büning-Pfaue, H. (2003). Analysis of water in food by near infrared spectroscopy. *Food Chemistry*, *82*(1), 107–115. https://doi.org/10.1016/S0308-8146(02)00583-6

Cheng, J.-H., & Sun, D.-W. (2015). Rapid quantification analysis and visualization of *Escherichia coli* loads in grass carp fish flesh by hyperspectral imaging method. *Food and Bioprocess Technology*, *8*(5), 951–959. https://doi.org/10.1007/s11947-014-1457-9

Chu, X., Wang, W., Ni, X., Li, C., & Li, Y. (2020). Classifying maize kernels naturally infected by fungi using near-infrared hyperspectral imaging. *Infrared Physics & Technology*, *105*, 103242.

Chung, S., & Yoon, S.-C. (2021). Detection of foreign materials on broiler breast meat using a fusion of visible near-infrared and short-wave infrared hyperspectral imaging. *Applied Sciences*, *11*(24), 11987. https://www.mdpi.com/2076-3417/11/24/11987

Cliver, D. O., Ellender, R. D., & Sobsey, M. D. (1983). Methods for detecting viruses in foods: Background and general principles. *Journal of Food Protection*, *46*(3), 248–259. https://doi.org/10.4315/0362-028x-46.3.248

Crichton, S., Shrestha, L., Hurlbert, A., & Sturm, B. (2018). Use of hyperspectral imaging for the prediction of moisture content and chromaticity of raw and pretreated apple slices during convection drying. *Drying Technology*, *36*(7), 804–816.

Cucci, C., & Casini, A. (2020). Chapter 3.8—Hyperspectral imaging for artworks investigation. In J. M. Amigo (Ed.), *Data handling in science and technology* (Vol., 32, pp. 583–604). Elsevier.

Dagnas, S., & Membré, J.-M. (2013). Predicting and preventing mold spoilage of food products. *Journal of Food Protection*, *76*(3), 538–551.

Dalgaard, P., Mejlholm, O., Christiansen, T., & Huss, H. H. (1997). Importance of *Photobacterium phosphoreum* in relation to spoilage of modified atmosphere-packed fish products. *Letters in Applied Microbiology*, *24*(5), 373–378.

De Boer, E., Zwartkruis-Nahuis, J., Wit, B., Huijsdens, X., De Neeling, A., Bosch, T., van Oosterom, R. A. A., & Heuvelink, A. (2009). Prevalence of methicillin-resistant *Staphylococcus aureus* in meat. *International Journal of Food Microbiology*, *134*(1–2), 52–56.

Del Fiore, A., Reverberi, M., Ricelli, A., Pinzari, F., Serranti, S., Fabbri, A. A., Bonifazi, G., & Fanelli, C. (2010). Early detection of toxigenic fungi on maize by hyperspectral imaging analysis. *International Journal of Food Microbiology*, *144*(1), 64–71. https://doi.org/10.1016/j.ijfoodmicro.2010.08.001

Díaz, R., Cervera, L., Fenollosa, S., Ávila, C., & Belenguer, J. (2011). Hyperspectral system for the detection of foreign bodies in meat products. *Procedia Engineering*, *25*, 313–316. https://doi.org/10.1016/j.proeng.2011.12.077

Duan, C., Chen, C., Khan, M. N., Liu, Y., Zhang, R., Lin, H., & Cao, L. (2014). Non-destructive determination of the total bacteria in flounder fillet by portable near infrared spectrometer. *Food Control*, *42*, 18–22. https://doi.org/10.1016/j.foodcont.2014.01.023

Duguid, J. P., & North, R. A. E. (1991). Eggs and salmonella food-poisoning: An evaluation. *Journal of Medical Microbiology*, *34*(2), 65–72. https://doi.org/10.1099/00222615-34-2-65

Estelles-Lopez, L., Ropodi, A., Pavlidis, D., Fotopoulou, J., Gkousari, C., Peyrodie, A., Panagou, E., Nychas, G.-J., & Mohareb, F. (2017). An automated ranking platform for machine learning regression models for meat spoilage prediction using multi-spectral imaging and metabolic profiling. *Food Research International*, *99*, 206–215.

Feng, Y.-Z., ElMasry, G., Sun, D.-W., Scannell, A. G. M., Walsh, D., & Morcy, N. (2013). Near-infrared hyperspectral imaging and partial least squares regression for rapid and reagentless determination of Enterobacteriaceae on chicken fillets. *Food Chemistry*, *138*(2), 1829–1836. https://doi.org/10.1016/j.foodchem.2012.11.040

Feng, Y.-Z., & Sun, D.-W. (2012). Application of hyperspectral imaging in food safety inspection and control: A review. *Critical Reviews in Food Science and Nutrition*, *52*(11), 1039–1058.

Feng, Y.-Z., Yu, W., Chen, W., Peng, K.-K., & Jia, G.-F. (2018). Invasive weed optimization for optimizing one-agar-for-all classification of bacterial colonies based on hyperspectral imaging. *Sensors and Actuators B: Chemical*, *269*, 264–270. https://doi.org/10.1016/j.snb.2018.05.008

Foca, G., Ferrari, C., Ulrici, A., Sciutto, G., Prati, S., Morandi, S., Brasca, M., Lavermicocca, P., Lanteri, S., & Oliveri, P. (2016). The potential of spectral and hyperspectral-imaging techniques for bacterial detection in food: A case study on lactic acid bacteria. *Talanta*, *153*, 111–119.

Fueyo, J. M., Mendoza, M. C., & Martin, M. C. (2005). Enterotoxins and toxic shock syndrome toxin in *Staphylococcus aureus* recovered from human nasal carriers and manually handled foods: Epidemiological and genetic findings. *Microbes and Infection*, *7*(2), 187–194.

Gardner, G. A. (1981). *Brochothrix thermosphacta (Microbacterium thermosphactum)* in the spoilage of meats: A reveiw. T. A. Roberts, G. Hobbs, J. H. B. Christian, N. Skovgaard (Eds.), *Psychrotrophic Microorganisms in Spoilage and Pathogenicity*, Academic Press, New York, pp. 139–173.

Garnier, L., Valence, F., & Mounier, J. (2017). Diversity and control of spoilage fungi in dairy products: An update. *Microorganisms*, *5*(3), 42.

Gibbons, K. P. (2014). *Hyperspectral imaging what is it? How does it work* Government Products Group, Deposition Sciences, Inc., [Online]. Available: Retrived from https://www.techbriefs.com/component/content/article/tb/features/application-briefs/19507

Gowen, A. A., O'Donnell, C. P., Cullen, P. J., Downey, G., & Frias, J. M. (2007). Hyperspectral imaging—An emerging process analytical tool for food quality and safety control. *Trends in Food Science & Technology*, *18*(12), 590–598. https://doi.org/10.1016/j.tifs.2007.06.001

Gram, L., & Melchiorsen, J. (1996). Interaction between fish spoilage bacteria *Pseudomonas* sp. and *Shewanella putrefaciens* in fish extracts and on fish tissue. *Journal of Applied Bacteriology*, *80*(6), 589–595.

Griffiths, M. W., & Schraft, H. (2017). Chapter 20—*Bacillus cereus* food poisoning. In C. E. R. Dodd, T. Aldsworth, R. A. Stein, D. O. Cliver, & H. P. Riemann (Eds.), *Foodborne diseases* (3rd ed., pp. 395–405). Academic Press.

Gu, Q., Sheng, L., Zhang, T., Lu, Y., Zhang, Z., Zheng, K., Hu, H., & Zhou, H. (2019). Early detection of tomato spotted wilt virus infection in tobacco using the hyperspectral imaging technique and machine learning algorithms. *Computers and Electronics in Agriculture*, *167*, 105066. https://doi.org/10.1016/j.compag.2019.105066

Hansman, G. S., Oka, T., Okamoto, R., Nishida, T., Toda, S., Noda, M., Sano, D., Ueki, Y., Imai, T., Omura, T., Nishio, O., Kimura, H., & Takeda, N. (2007). Human sapovirus in clams, Japan. *Emerging Infectious Diseases*, *13*(4), 620–622. https://doi.org/10.3201/eid1304.061390

He, Z., Williamson, N., Smith, C. D., Gragston, M., & Zhang, Z. (2020). Compressed single-shot hyperspectral imaging for combustion diagnostics. *Applied Optics*, *59*(17), 5226–5233. https://doi.org/10.1364/AO.390335

Huang, L., Zhao, J., Chen, Q., & Zhang, Y. (2013). Rapid detection of total viable count (TVC) in pork meat by hyperspectral imaging. *Food Research International*, *54*(1), 821–828. https://doi.org/10.1016/j.foodres.2013.08.011

Iritani, N., Kaida, A., Abe, N., Kubo, H., Sekiguchi, J.-I., Yamamoto, S. P., Goto, K., Tanaka, T., & Noda, M. (2014). Detection and genetic characterization of human enteric viruses in oyster-associated gastroenteritis outbreaks between 2001 and 2012 in Osaka City, Japan. *Journal of Medical Virology*, *86*(12), 2019–2025. https://doi.org/10.1002/jmv.23883

Islam, M. S., Sazzad, H. M., Satter, S. M., Sultana, S., Hossain, M. J., Hasan, M., Rahman, M., Campbell, S., Cannon, D. L., Ströher, U., Daszak, P., Luby, S. P., & Ströher, U. (2016). Nipah virus transmission from bats to humans associated with drinking traditional liquor made from date palm sap, Bangladesh, 2011–2014. *Emerging Infectious Diseases*, *22*(4), 664.

Jacobs-Reitsma, W., Lyhs, U., & Wagenaar, J. (2008). Campylobacter in the food supply. In *EINCMSAMJBE (ed.), Campylobacter*. ASM Press, Washington, DC, pp. 627–644.

Jami, M., Ghanbari, M., Zunabovic, M., Domig, K. J., & Kneifel, W. (2014). *Listeria monocytogenes* in aquatic food products—A review. *Comprehensive Reviews in Food Science and Food Safety*, *13*(5), 798–813. https://doi.org/10.1111/1541-4337.12092

Jespersen, L., & Jakobsen, M. (1996). Specific spoilage organisms in breweries and laboratory media for their detection. *International Journal of Food Microbiology*, *33*(1), 139–155.

Jia, B., Wang, W., Ni, X., Lawrence, K. C., Zhuang, H., Yoon, S.-C., & Gao, Z. (2020). Essential processing methods of hyperspectral images of agricultural and food products. *Chemometrics and Intelligent Laboratory Systems*, *198*, 103936.

Kang, Z., & Buchenauer, H. (2000). Cytology and ultrastructure of the infection of wheat spikes by *Fusarium culmorum*. *Mycological Research*, *104*(9), 1083–1093.

Kim, M. S., Chao, K., Chen, Y.-R., Chan, D., & Mehl, P. M. (2001), March. Hyperspectral imaging system for food safety: Detection of fecal contamination on apples [Paper presentation]. The Photonic Detection and Intervention Technologies for Safe Food, Boston, MA, United States.

Kim, M. S., Lefcourt, A. M., Chen, Y.-R., & Tao, Y. (2005). Automated detection of fecal contamination of apples based on multispectral fluorescence image fusion. *Journal of Food Engineering*, *71*(1), 85–91. https://doi.org/10.1016/j.jfoodeng.2004.10.022

Kobayashi, S., Fujiwara, N., Yasui, Y., Yamashita, T., Hiramatsu, R., & Minagawa, H. (2012). A foodborne outbreak of sapovirus linked to catered box lunches in Japan. *Archives of Virology*, *157*(10), 1995–1997. https://doi.org/10.1007/s00705-012-1394-8

Kodish, S. R., Bio, F., Oemcke, R., Conteh, J., Beauliere, J. M., Pyne-Bailey, S., Rohner, F., Ngnie-Teta, I., Jalloh, M. B., & Wirth, J. P. (2019). A qualitative study to understand how Ebola Virus Disease affected nutrition in Sierra Leone—A food value-chain framework for improving future response strategies. *PLoS Neglected Tropical Diseases*, *13*(9), e0007645.

Kong, B., & Ma, L. (2003). *Meat science and technology* (pp. 97–99). Chinese Light Industry Press.

Koopmans, M., & Duizer, E. (2004). Foodborne viruses: An emerging problem. *International Journal of Food Microbiology*, *90*(1), 23–41. https://doi.org/10.1016/S0168-1605(03)00169-7

Kure, C. F., & Skaar, I. (2019). The fungal problem in cheese industry. *Current Opinion in Food Science*, *29*, 14–19. https://doi.org/10.1016/j.cofs.2019.07.003

Kusumaningrum, H. D., Riboldi, G., Hazeleger, W. C., & Beumer, R. R. (2003). Survival of foodborne pathogens on stainless steel surfaces and cross-contamination to foods. *International Journal of Food Microbiology*, *85*(3), 227–236. https://doi.org/10.1016/S0168-1605(02)00540-8

Law, J. W., Ab Mutalib, N. S., Chan, K. G., & Lee, L. H. (2014). Rapid methods for the detection of foodborne bacterial pathogens: Principles, applications, advantages and limitations. *Frontiers in Microbiology*, *5*, 770. https://doi.org/10.3389/fmicb.2014.00770

Lawrence, K. C., Windham, W. R., Park, B., & Buhr, R. J. (2001). Hyperspectral imaging for poultry contaminant detection. *NIR News*, *12*(5), 3–6.

Lee, H., Kim, M. S., Qin, J., Park, E., Song, Y.-R., Oh, C.-S., & Cho, B.-K. (2017). Raman hyperspectral imaging for detection of watermelon seeds infected with *Acidovorax citrulli*. *Sensors (Switzerland)*, *17*(10), 2188. https://www.mdpi.com/1424-8220/17/10/2188

Lee, H. B., Patriarca, A., & Magan, N. (2015). Alternaria in food: Ecophysiology, mycotoxin production and toxicology. *Mycobiology*, *43*(2), 93–106. https://doi.org/10.5941/MYCO.2015.43.2.93

Li, J., Xue, L., Liu, M., Wang, X., & Luo, C. (2010). Hyperspectral imaging technology for determination of dichlorvos residue on the surface of navel orange. *Chinese Optics Letters*, *8*(11), 1050–1052.

Li, Q., Song, P., & Wen, J. (2019). Melamine and food safety: A 10-year review. *Current Opinion in Food Science*, *30*, 79–84. https://doi.org/10.1016/j.cofs.2019.05.008

Lim, J., Lee, A., Kang, J., Seo, Y., Kim, B., Kim, G., & Kim, S. M. (2020). Non-destructive detection of bone fragments embedded in meat using hyperspectral reflectance imaging technique. *Sensors (Switzerland)*, *20*(14), 4038. https://www.mdpi.com/1424-8220/20/14/4038

Liu, Y., Pu, H., & Sun, D.-W. (2017). Hyperspectral imaging technique for evaluating food quality and safety during various processes: A review of recent applications. *Trends in Food Science & Technology*, *69*, 25–35.

Lorenzo, J. M., Munekata, P. E., Dominguez, R., Pateiro, M., Saraiva, J. A., & Franco, D. (2018). Main groups of microorganisms of relevance for food safety and stability: General aspects and overall description. *Innovative Technologies for food preservation*, Academic Press, 53–107. https://doi.org/10.1016/B978-0-12-811031-7.00003-0

Louten, J. (2016). Virus replication. *In Essential human virology*, (pp. 49–70. Academic Press. https://doi.org/10.1016/B978-0-12-800947-5.00004-1

Lovett, J., Francis, D., & Hunt, J. (1987). *Listeria monocytogenes* in raw milk: Detection, incidence, and pathogenicity. *Journal of Food Protection*, *50*(3), 188–192.

MacDonald, S. L., Staid, M., Staid, M., & Cooper, M. L. (2016). Remote hyperspectral imaging of grapevine leafroll-associated virus 3 in cabernet sauvignon vineyards. *Computers and Electronics in Agriculture*, *130*, 109–117. https://doi.org/10.1016/j.compag.2016.10.003

Magwaza, L. S., Opara, U. L., Nieuwoudt, H., Cronje, P. J., Saeys, W., & Nicolaï, B. (2012). NIR spectroscopy applications for internal and external quality analysis of citrus fruit—A review. *Food and Bioprocess Technology*, *5*(2), 425–444.

Makun, H. A., Dutton, M. F., Njobeh, P. B., Mwanza, M., & Kabiru, A. Y. (2011). Natural multi-occurrence of mycotoxins in rice from Niger State, Nigeria. *Mycotoxin Research*, *27*(2), 97–104. https://doi.org/10.1007/s12550-010-0080-5

Marchese, S., Polo, A., Ariano, A., Velotto, S., Costantini, S., & Severino, L. (2018). Aflatoxin B1 and M1: Biological properties and their involvement in cancer development. *Toxins*, *10*(6), 214. https://www.mdpi.com/2072-6651/10/6/214

Marshall, S., Kelman, T., Qiao, T., Murray, P., & Zabalza, J. (2015), August 31–September 4. *Hyperspectral imaging for food applications* [Paper presentation]. The 2015 23rd European Signal Processing Conference (EUSIPCO), Nice, France.

Martin, N. H., Murphy, S. C., Ralyea, R. D., Wiedmann, M., & Boor, K. J. (2011). When cheese gets the blues: *Pseudomonas fluorescens* as the causative agent of cheese spoilage. *Journal of Dairy Science*, *94*(6), 3176–3183. https://doi.org/10.3168/jds.2011-4312

Martinović, T., Andjelković, U., Gajdošik, M. Š., Rešetar, D., & Josić, D. (2016). Foodborne pathogens and their toxins. *Journal of Proteomics*, *147*, 226–235. https://doi.org/10.1016/j.jprot.2016.04.029

McCormick, S. (2003). The role of DON in pathogenicity. In *Fusarium head blight of wheat and barley*, (pp. 165–183). American Phytopathological Society (APS Press).

Meyer, C., Thiel, S., Ullrich, U., & Stolle, A. (2010). *Salmonella* in raw meat and by-products from pork and beef. *Journal of Food Protection*, *73*(10), 1780–1784. https://doi.org/10.4315/0362-028x-73.10.1780

Michael, M., Phebus, R. K., & Amamcharla, J. (2019). Hyperspectral imaging of common foodborne pathogens for rapid identification and differentiation. *Food Science & Nutrition*, *7*(8), 2716–2725. https://doi.org/10.1002/fsn3.1131

Misra, N., Dixit, Y., Al-Mallahi, A., Bhullar, M. S., Upadhyay, R., & Martynenko, A. (2022). IoT, big data and artificial intelligence in agriculture and food industry. *IEEE Internet of Things Journal*, *9*, 6305–6324.

Nguyen, C., Sagan, V., Maimaitiyiming, M., Maimaitijiang, M., Bhadra, S., & Kwasniewski, M. T. (2021). Early detection of plant viral disease using hyperspectral imaging and deep learning. *Sensors (Switzerland)*, *21*(3), 742. https://www.mdpi.com/1424-8220/21/3/742

Nieminen, T. T., Dalgaard, P., & Björkroth, J. (2016). Volatile organic compounds and *Photobacterium phosphoreum* associated with spoilage of modified-atmosphere-packaged raw pork. *International Journal of Food Microbiology*, *218*, 86–95.

Oh, S. K., Lee, N., Cho, Y. S., Shin, D.-B., Choi, S. Y., & Koo, M. (2007). Occurrence of toxigenic *Staphylococcus aureus* in ready-to-eat food in Korea. *Journal of Food Protection*, *70*(5), 1153–1158.

Okull, D. O., Demirci, A., Rosenberger, D., & Laborde, I. F. (2006). Susceptibility of *Penicillium expansum* spores to sodium hypochlorite, electrolyzed oxidizing water, and chlorine dioxide solutions modified with nonionic surfactants. *Journal of Food Protection*, *69*(8), 1944–1948. https://doi.org/10.4315/0362-028x-69.8.1944

Oliver, S. P., Boor, K. J., Murphy, S. C., & Murinda, S. E. (2009). Food safety hazards associated with consumption of raw milk. *Foodborne Pathogens and Disease*, *6*(7), 793–806.

Onyekuru, N. A., Ume, C. O., Ezea, C. P., & Ume, N. N. C. (2020). Effects of Ebola virus disease outbreak on bush meat enterprise and environmental health risk behavior among households in south-east Nigeria. *The Journal of Primary Prevention*, *41*(6), 603–618.

Ozdemir, A., & Polat, K. (2020). Deep learning applications for hyperspectral imaging: A systematic review. *Journal of the Institute of Electronics and Computer*, *2*(1), 39–56.

Parashar, U. D., Sunn, L. M., Ong, F., Mounts, A. W., Arif, M. T., Ksiazek, T. G., Kamaluddin, M. A., Mustafa, A. N., Kaur, H., Ding, L. M., Othman, G., Radzi, H. M., Kitsutani, P. T., Stockton, P. C., Arokiasamy, J., Gary, H. E. Jr., & Anderson, L. J. (2000). Case-control study of risk factors for human infection with a new zoonotic Paramyxovirus, Nipah Virus, during a 1998–1999 outbreak of severe encephalitis in Malaysia. *The Journal of Infectious Diseases*, *181*(5), 1755–1759. https://doi.org/10.1086/315457

Park, B., Windham, W. R., Ladely, S. R., Gurram, P., Kwon, H., Yoon, S.-C., Lawrence, K. C., Neelam, N., & Cray, W. C. (2012), May 4. *Classification of Shiga toxin-producing Escherichia coli (STEC) serotypes with hyperspectral microscope imagery* [Paper presentation]. The Sensing for Agriculture and Food Quality and Safety IV, Baltimore, MD, United States.

Peck, M. W. (2006). *Clostridium botulinum* and the safety of minimally heated, chilled foods: An emerging issue? *Journal of Applied Microbiology*, *101*(3), 556–570. https://doi.org/10.1111/j.1365-2672.2006.02987.x

Pei, X., Yang, S., Zhan, L., Zhu, J., Song, X., Hu, X., Liu, G., Ma, G., li, N., & Yang, D. (2018). Prevalence of *Bacillus cereus* in powdered infant and powdered follow-up formula in China. *Food Control*, *93*, 101–105.

Penner, M. H. (2017). Basic principles of spectroscopy. In *Food analysis* (pp. 79–88.) Springer.

Pérez-Torrado, R., & Querol, A. (2016). Opportunistic strains of *Saccharomyces cerevisiae*: A potential risk sold in food products. *Frontiers in Microbiology*, *6*, 1522. https://doi.org/10.3389/fmicb.2015.01522

Petrović, T., & D'Agostino, M. (2016). Viral contamination of food. In *Antimicrobial food packaging*, (pp. 65–79). Academic Press. https://doi.org/10.1016/B978-0-12-800723-5.00005-X

Pintó, R. M., & Bosch, A. (2008). Rethinking virus detection in food. In *Food-borne viruses* (pp. 171–188.).

Polder, G., Blok, P. M., de Villiers, H. A. C., van der Wolf, J. M., & Kamp, J. (2019). Potato Virus Y detection in seed potatoes using deep learning on hyperspectral images. *Frontiers in Plant Science*, *10*, 209. https://www.frontiersin.org/article/10.3389/fpls.2019.00209

Priore, R. J., Olkhovyk, O., Drauch, A., Treado, P., Kim, M., & Chao, K. (2009), April 27. *Recent advances in chemical imaging technology for the detection of contaminants for food safety and security* [Paper presentation]. The Sensing for Agriculture and Food Quality and Safety, Orlando, FL, United States.

Pu, Y.-Y., Feng, Y.-Z., & Sun, D.-W. (2015). Recent progress of hyperspectral imaging on quality and safety inspection of fruits and vegetables: A review. *Comprehensive Reviews in Food Science and Food Safety*, *14*(2), 176–188. https://doi.org/10.1111/1541-4337.12123

Raposo, A., Pérez, E., de Faria, C. T., Ferrús, M. A., & Carrascosa, C. (2016). Food spoilage by *Pseudomonas* spp.—An overview. In *Foodborne pathogens and antibiotic resistance*, (pp. 41–71). John Wiley & Sons, Incorporated.

Ren, J., Zabalza, J., Marshall, R. T., & Zheng, J. (2014). Effective feature extraction and data reduction in remote sensing using hyperspectral imaging [Applications Corner]. *IEEE Signal Processing Magazine*, *31*(4), 149–154. https://doi.org/10.1109/MSP.2014.2312071

Rodrigues, E. M., Rutajoga, N., Rioux, D., Yvon-Leroux, J., & Hemmer, E. (2020). Hyperspectral imaging as a tool to study optical anisotropy in lanthanide-based molecular single crystals. JoVE, 158, e60826. https://doi.org/10.3791/60826

Rusul, G., & Yaacob, N. H. (1995). Prevalence of *Bacillus cereus* in selected foods and detection of enterotoxin using TECRA-VIA and BCET-RPLA. *International Journal of Food Microbiology*, *25*(2), 131–139. https://doi.org/10.1016/0168-1605(94)00086-L

Ryser, E. T., Arimi, S. M., Bunduki, M., & Donnelly, C. W. (1996). Recovery of different *Listeria* ribotypes from naturally contaminated, raw refrigerated meat and poultry products with two primary enrichment media. *Applied and Environmental Microbiology*, *62*(5), 1781–1787.

Saleh, I., & Al-Thani, R. (2019). Fungal food spoilage of supermarkets' displayed fruits. *Veterinary World*, *12*(11), 1877–1883. https://doi.org/10.14202/vetworld.2019.1877-1883

Saw, S., Mak, J., Tan, M., Teo, S., Tan, T., Cheow, M., Ong, C. A., Chen, S.-N., Yeo, S.-K., Kuan, C. S., New, C. Y., Radu, S., Phuah, E.-T., Thung, T. Y., & Kuan, C. (2020). Detection and quantification of *Salmonella* in fresh vegetables in perak, Malaysia. *Food Research*, *4*(2), 441–448.

Seo, Y.-H., Jang, J.-H., & Moon, K.-D. (2010). Occurrence and characterization of enterotoxigenic *Staphylococcus aureus* isolated from minimally processed vegetables and sprouts in Korea. *Food Science and Biotechnology*, *19*(2), 313–319.

Sharma, K., & Paradakar, M. (2010). The melamine adulteration scandal. *Food Security*, *2*(1), 97–107. https://doi.org/10.1007/s12571-009-0048-5

Sibanda, N., McKenna, A., Richmond, A., Ricke, S. C., Callaway, T., Stratakos, A. C., Gundogdu, O., & Corcionivoschi, N. (2018). A review of the effect of management practices on *Campylobacter* prevalence in poultry farms. *Frontiers in Microbiology*, *9*(2002), https://doi.org/10.3389/fmicb.2018.02002

Siche, R., Vejarano, R., Aredo, V., Velasquez, L., Saldana, E., & Quevedo, R. (2016). Evaluation of food quality and safety with hyperspectral imaging (HSI). *Food Engineering Reviews*, *8*(3), 306–322.

Snyder, A. B., Churey, J. J., & Worobo, R. W. (2019). Association of fungal genera from spoiled processed foods with physicochemical food properties and processing conditions. *Food Microbiology*, *83*, 211–218. https://doi.org/10.1016/j.fm.2019.05.012

Snyder, A. B., & Worobo, R. W. (2018). Fungal spoilage in food processing. *Journal of Food Protection*, *81*(6), 1035–1040.

Soltan Dallal, M. M., Sharifi Yazdi, M. K., Mirzaei, N., & Kalantar, E. (2014). Prevalence of *Salmonella* spp. in packed and unpacked red meat and chicken in south of Tehran. *Jundishapur Journal of Microbiology*, *7*(4), e9254–e9254. https://doi.org/10.5812/jjm.9254

Soni, A., Al-Sarayreh, M., Reis, M. M., & Brightwell, G. (2021). Hyperspectral imaging and deep learning for quantification of *Clostridium sporogenes* spores in food products using 1D-convolutional neural networks and random forest model. *Food Research International*, *147*, 110577. https://doi.org/10.1016/j.foodres.2021.110577

Soni, A., Oey, I., Silcock, P., & Bremer, P. (2016). *Bacillus* spores in the food industry: A review on resistance and response to novel inactivation technologies. *Comprehensive Reviews in Food Science and Food Safety*, *15*(6), 1139–1148. https://doi.org/10.1111/1541-4337.12231

Stals, A., Baert, L., Van Coillie, E., & Uyttendaele, M. (2012). Extraction of food-borne viruses from food samples: A review. *International Journal of Food Microbiology*, *153*(1), 1–9. https://doi.org/10.1016/j.ijfoodmicro.2011.10.014

Stepanchuk, A., Tahir, W., Nilsson, K. P. R., Schatzl, H. M., & Stys, P. K. (2021). Early detection of prion protein aggregation with a fluorescent pentameric oligothiophene probe using spectral confocal microscopy. *Journal of Neurochemistry*, *156*(6), 1033–1048. https://doi.org/10.1111/jnc.15148

Suchorab, Z., Frąc, M., Guz, Ł., Oszust, K., Łagód, G., Gryta, A., Bilińska-Wielgus, N., & Czerwiński, J. (2019). A method for early detection and identification of fungal contamination of building materials using e-nose. *Plos One*, *14*(4), e0215179–e0215179. https://doi.org/10.1371/journal.pone.0215179

Tang, B.-C., Cai, C.-B., Shi, W., & Xu, L. (2016). Rapid quantification of melamine in different brands/types of milk powders using standard addition net analyte signal and near-infrared spectroscopy. *Journal of Analytical Methods in Chemistry*, *2016*, 1–9.

Tsuta, M., El Masry, G., Sugiyama, T., Fujita, K., & Sugiyama, J. (2009), April 22–24. *Comparison between linear discrimination analysis and support vector machine for detection of pesticide on spinach leaf by hyperspectral imaging with excitation-emission matrix* [Paper presentation]. ESANN, Bruges, Belgium.

Tsuta, M., Takao, T., Junichi, S., Wada, Y., & Sagara, Y. (2006). Foreign substance detection in blueberry fruits by spectral imaging. *Food Science and Technology Research*, *12*(2), 96–100.

Turner, P. C., Flannery, B., Isitt, C., Ali, M., & Pestka, J. (2012). The role of biomarkers in evaluating human health concerns from fungal contaminants in food. *Nutrition Research Reviews*, *25*(1), 162–179. https://doi.org/10.1017/S095442241200008X

Turra, G., Conti, N., & Signoroni, A. (2015). Hyperspectral image acquisition and analysis of cultured bacteria for the discrimination of urinary tract infections. *Annual International Conference of the IEEE Engineering in Medicine and Biology Society*, *2015*, 759–762. https://doi.org/10.1109/embc.2015.7318473

Tuttle, J., Gomez, T., Doyle, M., Wells, J., Zhao, T., Tauxe, R., & Griffin, P. (1999). Lessons from a large outbreak of *Escherichia coli* O157 [ratio] H7 infections: Insights into the infectious dose and method of widespread contamination of hamburger patties. *Epidemiology & Infection*, *122*(2), 185–192.

Urbanos, G., Martín, A., Vázquez, G., Villanueva, M., Villa, M., Jimenez-Roldan, L., Chavarrías, M., Lagares, A., Juárez, E., & Sanz, C. (2021). Supervised machine learning methods and hyperspectral imaging techniques jointly applied for brain cancer classification. *Sensors (Switzerland)*, *21*(11), 3827. https://www.mdpi.com/1424-8220/21/11/3827

Van der Poel, W. H. M. (2014). Food and environmental routes of Hepatitis E virus transmission. *Current Opinion in Virology*, *4*, 91–96. https://doi.org/10.1016/j.coviro.2014.01.006

Vargas, A. M., Kim, M. S., Tao, Y., Lefcourt, A., & Chen, Y.-R. (2004), August 1–4. *Safety inspection of cantaloupes and strawberries using multispectral fluorescence imaging techniques* [Paper presentation]. The 2004 ASAE Annual Meeting, Ottawa, Canada.

Vázquez-Boland, J. A., Kuhn, M., Berche, P., Chakraborty, T., Domínguez-Bernal, G., Goebel, W., González-Zorn, B., & Kreft, J. R. (2001). *Listeria* pathogenesis and molecular virulence determinants. *Clinical Microbiology Reviews*, *14*(3), 584–640.

Veldman, A., Meijs, J., Borggreve, G., & Heeres-Van Der Tol, J. (1992). Carry-over of aflatoxin from cows' food to milk. *Animal Science*, *55*(2), 163–168.

Vidal, M., & Amigo, J. M. (2012). Pre-processing of hyperspectral images. Essential steps before image analysis. *Chemometrics and Intelligent Laboratory Systems*, *117*, 138–148. https://doi.org/10.1016/j.chemolab.2012.05.009

Vieira, K. C. D. O., Silva, H. R. A. D., Rocha, I. P. M., Barboza, E., & Eller, L. K. W. (2021). Foodborne pathogens in the omics era. *Critical Reviews in Food Science and Nutrition*, 1–16.

Wang, D., Vinson, R., Holmes, M., Seibel, G., Bechar, A., Nof, S., & Tao, Y. (2019). Early detection of tomato spotted wilt virus by hyperspectral imaging and outlier removal auxiliary classifier generative adversarial nets (OR-AC-GAN). *Scientific Reports*, *9*(1), 4377. https://doi.org/10.1038/s41598-019-40066-y

Wedemeyer, H., Pischke, S., & Manns, M. P. (2012). Pathogenesis and treatment of Hepatitis E virus infection. *Gastroenterology*, *142*(6), 1388–1397.e1381. https://doi.org/10.1053/j.gastro.2012.02.014

Wu, D., & Sun, D.-W. (2013). Advanced applications of hyperspectral imaging technology for food quality and safety analysis and assessment: A review—Part I: Fundamentals. *Innovative Food Science & Emerging Technologies*, *19*, 1–14. https://doi.org/10.1016/j.ifset.2013.04.014

Wu, F., Groopman, J. D., & Pestka, J. J. (2014). Public health impacts of foodborne mycotoxins. *Annual Review of Food Science and Technology*, *5*, 351–372.

Wu, Y.-N., Zhao, Y.-F., & Li, J.-G. (2009). A Survey on occurrence of melamine and its analogues in tainted infant formula in China. *Biomedical and Environmental Sciences*, *22*(2), 95–99. https://doi.org/10.1016/S0895-3988(09)60028-3

Xia, Z., Zhang, C., Weng, H., Nie, P., & He, Y. (2017). Sensitive wavelengths selection in identification of *Ophiopogon japonicus* based on near-infrared hyperspectral imaging technology. *International Journal of Analytical Chemistry*, *2017*, 6018769–6018769. https://doi.org/10.1155/2017/6018769

Xu, Y. Z., Anyogu, A., Ouoba, L., & Sutherland, J. (2010). Genotypic characterization of *Brochothrix* spp. isolated from meat, poultry and fish. *Letters in Applied Microbiology*, *51*(3), 245–251.

Yang, C.-C., Jun, W., Kim, M. S., Chao, K., Kang, S., Chan, D. E., & Lefcourt, A. (2010), April 26). *Classification of fecal contamination on leafy greens by hyperspectral imaging* [Paper presentation]. The Sensing for Agriculture and Food Quality and Safety II, Orlando, FL, United States.

Zastempowska, E., Grajewski, J., & Twaruzek, M. (2016). Food-borne pathogens and contaminants in raw milk—A review. *Annals of Animal Science*, *16*(3), 623.

Zhang, H., Paliwal, J., Jayas, D. S., & White, N. (2007). Classification of fungal infected wheat kernels using near-infrared reflectance hyperspectral imaging and support vector machine. *Transactions of the ASABE*, *50*(5), 1779–1785.

Zhang, X., Liu, F., He, Y., & Gong, X. (2013). Detecting macronutrients content and distribution in oilseed rape leaves based on hyperspectral imaging. *Biosystems Engineering*, *115*(1), 56–65. https://doi.org/10.1016/j.biosystemseng.2013.02.007

Zhang, Y., & Mathys, A. (2019). Superdormant spores as a hurdle for gentle germination-inactivation based spore control strategies. *Frontiers in Microbiology*, *9*, 3163. https://doi.org/10.3389/fmicb.2018.03163

Zöllner, P., & Mayer-Helm, B. (2006). Trace mycotoxin analysis in complex biological and food matrices by liquid chromatography–atmospheric pressure ionisation mass spectrometry. *Journal of Chromatography A*, *1136*(2), 123–169.

How to cite this article: Soni, A., Dixit, Y., Reis, M. M., & Brightwell, G. (2022). Hyperspectral imaging and machine learning in food microbiology: Developments and challenges in detection of bacterial, fungal, and viral contaminants. *Comprehensive Reviews in Food Science and Food Safety*, *21,* 3717–3745. https://doi.org/10.1111/1541-4337.12983